Three Dimensional Nonlinear Dynamics of Slender Structures: Cosserat Rod Element Approach

D. Q. Cao*, Dongsheng Liu and Charles H.-T. Wang†

Department of Physics, Lancaster University, Lancaster LA1 4YB, UK

Abstract

In this paper, the modelling strategy of a Cosserat rod element (CRE) is addressed systematically for 3-dimensional dynamical analysis of slender structures. We employ the exact nonlinear kinematic relationships in the sense of Cosserat theory, and adopt the Bernoulli hypothesis. For the sake of simplicity, the Kirchoff constitutive relations are adopted to provide an adequate description of elastic properties in terms of a few elastic moduli. A deformed configuration of the rod is described by the displacement vector of the deformed centroid curves and an orthonormal moving frame, rigidly attached to the cross-section of the rod. The position of the moving frame relative to the inertial frame is specified by the rotation matrix, parametrized by a rotational vector. The approximate solutions of the nonlinear partial differential equations of motion in quasi-static sense are chosen as the shape functions with up to third order nonlinear terms of generic nodal displacements. Based on the Lagrangian constructed by the Cosserat kinetic energy and strain energy expressions, the principle of virtual work is employed to derive the ordinary differential equations of motion with third order nonlinear generic nodal displacements. A simple example is presented to illustrate the use of the formulation developed here to obtain the lower order nonlinear ordinary differential equations of motion of a given structure. The corresponding nonlinear dynamical responses of the structures have been presented through numerical simulations by Matlab software.

Keywords: Cosserat rod element; Cosserat theory; Three-dimensional rotation; Multibody systems; Nonlinear dynamic model

*Corresponding Author. Email: d.cao@lancaster.ac.uk (DQ Cao)

†Permanent address starting 1 Jan 2005: School of Engineering and Physical Sciences, University of Aberdeen, Aberdeen AB24 3UE, Scotland

1 Introduction

Three-dimensional slender structures undergoing large displacements and rotations are often encountered in various engineering systems such as vehicles, space structures, robotics, aircrafts, and microelectronic mechanical systems. Clearly, these systems consist of a set of interconnected components which may be rigid or deformable. For example, a typical MEMS device may consist of relatively heavy load bodies and thin springlike supports. For such a system, each heavy body can be assumed to be a rigid body and each springlike component can be described as a deformable body. Since each of interconnected components of such a system may undergo large displacements and/or rotations, an effective modelling strategy that addresses very well to the strongly nonlinear dynamic behavior is crucial in estimating system performance and guiding the reliability verification process.

Nonlinear finite element method provides a general approach to structural modelling of multibody systems that consist of interconnected *rigid* and *deformable* components. A number of papers has recently been published, presenting new concepts and new algorithms for modelling highly flexible spatial frame structures [1, 2, 3]. An overview and comprehensive treatment of this topic can be found, for instance, in [4, 5]. The Cosserat approach, that can accommodate a good approximation the nonlinear behavior of complex structures composed of materials with different constitutive properties, variable geometry and damping characteristics [6, 7, 8, 9], has been utilized to develop finite element formulations for deformable bodies. The finite element approach based on the Cosserat theory (geometrically exact finite-strain beam theory) is usually attributed to Reissner [10] and Simo [11]. Simo [11] has discussed a convenient parameterization of the rod model developed by Antman [12], and Simo and Vu-Quoc [13] have considered the associated finite element formulation. The computational procedure in [13] uses a variational formulation of the equations of motion and an expansion of the kinematic quantities in terms of shape functions and nodal values. Many modern finite element developers of the three-dimensional beam theories, e.g. Jelenic and Saje [14], Smolenski [15], and Zupan and Saje [16] based their approach on the geometrically exact beam theory. Another approach based on a system of Cosserat-type bodies can be traced back to the work of Wozniak [17]. Homogeneously deformable bodies have been analyzed as pseudo-rigid bodies [18] and Cosserat points [19]. The theory of a Cosserat point is a special continuum theory that models deformation of a small structure that is essentially a point surrounded by some small but finite region. The numerical procedure based on the theory of a Cosserat point proposed in [19, 20] has been used to study the dynamics of spherically symmetric problems in [21]. Recently, the theory of a Cosserat point has been generalized to model a fully nonlinear finite element for the numerical solution

of 3-D dynamic problems of elastic beams [22].

However, in practice the use of FEM codes to simulate complex multibody systems such as MEMS devices is prohibitively cumbersome, expensive, and time consuming. On the other hand, FEM models use numerous variables to describe the device state. This may lead the process of mapping the design space complex and the relationship between each of these variables and the overall device performance is not clear to designers. Recently, component level modelling methods, which contain a library of parameterised behavioural models for frequently used MEMS components [23, 24], have been developed. In [23, 24], every component is described as a single element in contrast to FE models where the component is normally discretised into many elements. Consequently, lower degree models are established and the simulation time can be greatly reduced. The mechanical behaviour of the components, however, is often modelled using basic models, containing e.g. linear stiffness relationships and/or approximations of basic nonlinearities.

Recently, motivated by the developments in MEMS modelling, the Cosserat theory has been employed to develop a novel modelling strategy that addresses very well to the practical needs for rapid modelling of slender structures such as the springlike components in MEMS, see Wang *et al.* [25]. This modelling strategy has been successfully used to investigate the non-ideal properties of typical MEMS beams [26]. In the sense of Cosserat theory, the motion of rods in three-dimensional space can be demonstrated by behaviors of a reference curve and three perpendicular unit vectors (directors). Consequently, the equations of motion are nonlinear partial differential equations, which are functions of time and one space variable. For static problems, however, the equations become nonlinear ordinary differential equations, which can be solved approximately using standard techniques like the perturbation method to satisfy boundary conditions. In contrast, for dynamical problems, it is necessary to introduce a numerical procedure which discretizes the equations. In the strategy for modelling of a Cosserat rod element [25], the basic kinematic quantities are the position of a point on the Cosserat curve and an orthogonal transformation that define the rotation of an orthogonal triad attached to the cross-section at each point of the Cosserat curve. This enables description of a rod using nonlinear ordinary differential equations in terms of the generic nodal displacements of a CRE.

As an initial consideration, the modelling strategy in [25] is developed for 2-D case. In this paper, the modelling strategy of CRE is addressed systematically for the 3-D problems. The fundamental problem of any finite element formulation is the choice of the shape functions. The approximate solutions of the nonlinear equations of motion in quasi-static sense are chosen as the shape functions with up to

third order nonlinear terms of generic nodal displacements. In three dimensions, the nonlinear differential equations cannot be integrated in a closed form even in the static sense, therefore the perturbation method is employed here to solve the system approximately. For the sake of simplicity, the Kirchoff constitutive relations are adopted to provide an adequate description of elastic properties in terms of a few elastic moduli. Based on the Lagrangian constructed by the Cosserat kinetic energy and strain energy expressions, the principle of virtual work is used to derive the ordinary differential equations of motion with third order nonlinear generic nodal displacements. The essential features and novel aspects of the present formulation for CREs are briefly summarized below.

1. The shape functions for CREs are derived from the differential equations governing the flexural-flexural-torsional motion of extensional rods, taking into account all the geometric nonlinearities in the system. Consequently, the higher accuracy of the dynamic responses can be achieved by dividing the rod into a few elements which is much less than the traditional finite element methods in which the interpolation functions are usually extremely simple functions such as low order polynomials.

2. The mathematical simplicity when formulating deformable bodies enables more convenient for modelling the multibody systems that consist of interconnected *rigid* and *deformable* components.

3. The resulting nonlinear ordinary differential equations with lower degree-of-freedom are typically easy to simulate or integrate into system-level simulations.

An outline of the main contents of this paper is as follows. We begin in section 2 by introducing the basic definitions and kinematic assumptions on the nonlinear elastic rods that can suffer flexure, extension, torsion, and shear. The rotational vector that is free both of singularities and constraints is employed as a parametrization to specify the deformed configuration space. We limited our attention here to the modelling of Cosserat rod elements in which the small effect of shear will be neglected. The governing equations of motion and the Kirchoff constitutive relations are presented in Section 3. The straightforward perturbation method is employed in Section 4 to solve the corresponding static problem. The approximate solutions obtained are subsequently used as shape functions of Cosserat rod elements. In section 5, Lagrangian approach is employed to formulate the nonlinear ordinary differential equations of motion of Cosserat rod elements. In terms of the shape functions derived in Section 4, the Lagrangian is constructed by the Cosserat kinetic energy and strain energy expressions, and the virtual work done by external point loads and distributed loads is discussed. A simple example is presented in section

7 to illustrate the use of the formulation developed here to obtain the lower order nonlinear ordinary differential equations of motion of a given structure. The corresponding nonlinear dynamical responses of the structure have been presented through numerical simulations by Matlab software.

The following conventions and nomenclature will be used through out this paper. Vectors, which are elements of Euclidean 3-space $\mathscr{R}^3$, are denoted by lowercase, bold-face symbols, e.g., $\mathbf{u}$, $\mathbf{v}$; vector-valued functions are denoted by lowercase, italic, bold-face symbols, e.g., $\boldsymbol{u}$, $\boldsymbol{v}$; tensors are denoted by upper-case, bold-face symbols, e.g., $\mathbf{I}$, $\mathbf{J}$; matrices are denoted by upper-case, italic, bold-face symbols, e.g., $\boldsymbol{M}$, $\boldsymbol{K}$. The three vectors $\{\mathbf{e}_1, \mathbf{e}_2, \mathbf{e}_3\}$ are assumed to form a fixed right-handed orthogonal basis. The summation convention for repeated indices is used. The symbols ∂_t and ∂_s denote differentiation with respect to time t and arc-length parameter s, respectively. The symbols $(\dot{})$ and $(')$ denote differentiation with respect to dimensionless time parameter τ and dimensionless length parameter σ, respectively.

2 Kinematical Preliminaries

2.1 Basic definitions and kinematic assumptions

Adopt Cartesian coordinates (x, y, z) in inertial basis $(\mathbf{e}_1, \mathbf{e}_2, \mathbf{e}_3)$ with Newtonian time t. According to the Bernoulli hypothesis the plane cross-sections suffer only rigid rotation during deformation and remain plane after deformation and preserve their shape and area. For the sake of convenience, we introduce the following definitions: (1) the reference configuration, where the geometrical and mechanical variables of the rod, including the loading, are known; (2) an arbitrary deformed configuration, where only the loading is prescribed, while the remaining variables are unknown.

It is therefore convenient to introduce an orthonormal basis $\mathbf{d}_i(s,t), (i = 1, 2, 3)$ of a cross-section at s, termed the moving basis, such that $\mathbf{d}_3$ is normal to the rotated cross-section, and $\mathbf{d}_1$ and $\mathbf{d}_2$ lie in the plane of the rotated cross-section. The motion of a rod segment can be modelled as a Cosserat rod whose configuration is described by its neutral axis $\mathbf{r}(s,t)$ (Cosserat curve) and 3 orthogonal unit vectors $\mathbf{d}_i(s,t), (i = 1, 2, 3)$ (Cosserat directors) as shown in Figure 1.

At any time, $\mathbf{r}$ describes the axis of the rod whose cross-section orientations are determined by $\mathbf{d}_i$ such that $\partial_s \mathbf{r} \cdot \mathbf{d}_3 > 0$. This condition implies that (i) the local ration of deformed length to reference length of the axis cannot be reduced to zero since $|\partial_s \mathbf{r}| > 0$, and (ii) a typical cross-section ($s = s_0$) cannot

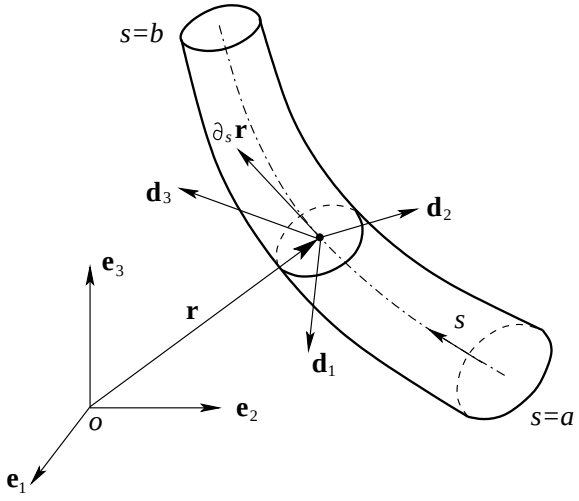

Figure 1: A simple Cosserat model

undergo a total shear in which the plane determined by $\mathbf{d}_1$ and $\mathbf{d}_2$ is tangent to the curve $\mathbf{r}(\cdot, t)$ at $\mathbf{r}(s_0, t)$ [10]. In general, as a result of shear deformations of the rod, the cross-sections are not perpendicular to the line of centroids.

In an inertial Cartesian basis $\{\mathbf{e}_1, \mathbf{e}_2, \mathbf{e}_3\}$ we may write

$$\mathbf{r}(s,t) = r_i(s,t)\,\mathbf{e}_i = x(s,t)\mathbf{e}_1 + y(s,t)\mathbf{e}_2 + z(s,t)\mathbf{e}_3. \tag{1}$$

The motion involves both the velocity of the curve, $\partial_t \mathbf{r}(s,t)$, and angular velocity of the cross-sections $\mathbf{w}(s,t)$ so that

$$\partial_t \mathbf{d}_i(s,t) = \mathbf{w}(s,t) \times \mathbf{d}_i(s,t). \tag{2}$$

In a similar manner the strains of the Cosserat rod are classified into "linear strain" vector $\mathbf{v}(s,t) = \partial_s \mathbf{r}(s,t)$ and "angular strain" vector $\mathbf{u}(s,t)$ so that

$$\partial_s \mathbf{d}_i(s,t) = \mathbf{u}(s,t) \times \mathbf{d}_i(s,t). \tag{3}$$

It follows from the definition (2) that

$$\mathbf{d}_i \times \partial_t \mathbf{d}_i = \mathbf{d}_i \times (\mathbf{w} \times \mathbf{d}_i) = \mathbf{w}(\mathbf{d}_i \cdot \mathbf{d}_i) - \mathbf{d}_i(\mathbf{d}_i \cdot \mathbf{w}) = 2\mathbf{w}.$$

Therefore,

$$\mathbf{w} = \frac{1}{2}\,\mathbf{d}_i \times \partial_t \mathbf{d}_i. \tag{4}$$

Similarly, from the definition (3) we have

$$\mathbf{u} = \frac{1}{2}\,\mathbf{d}_i \times \partial_s \mathbf{d}_i. \tag{5}$$

Since the basis $\{\mathbf{d}_1, \mathbf{d}_2, \mathbf{d}_3\}$ is natural for the intrinsic description of deformation, we decompose relevant vector valued functions with respect to it:

$$\mathbf{v}(s,t) = v_i(s,t)\mathbf{d}_i(s,t), \qquad \mathbf{u}(s,t) = u_i\mathbf{d}_i(s,t), \qquad \mathbf{w}(s,t) = w_i\mathbf{d}_i(s,t). \tag{6}$$

2.2 Parametrization of the rotation matrix

There is a number of choices for the parametrization of rotation matrix, for example, the Euler angles, the quaternion parameters, and the rotational vector being the most usual [27]. Here, we employ the rotational vector that is free both of singularities and constraints. Because of the orthogonality the rotation matrix is a proper orthogonal matrix in SO(3), its nine components can be expressed by only three independent parameters. Denote $\boldsymbol{S}$ the spin matrix of a vector $\mathbf{a} = a_i\mathbf{e}_i$ as

$$\boldsymbol{S}(\mathbf{a}) = \begin{bmatrix} 0 & -a_3 & a_2 \\ a_3 & 0 & -a_1 \\ -a_2 & a_1 & 0 \end{bmatrix}. \tag{7}$$

Then, the rotation matrix $\boldsymbol{R}$ is determined by the expression [27]

$$\boldsymbol{R}(\boldsymbol{\phi}) = \boldsymbol{I} + \frac{\sin\phi}{\phi}\boldsymbol{S}(\boldsymbol{\phi}) + \frac{1-\cos\phi}{\phi^2}\boldsymbol{S}^2(\boldsymbol{\phi}), \tag{8}$$

where $\boldsymbol{\phi} = \phi_i\mathbf{e}_i$ is the rotational vector, $\boldsymbol{S}(\boldsymbol{\phi})$ is the spin matrix of $\boldsymbol{\phi}$ defined by (7), and $\phi = (\phi_1^2 + \phi_2^2 + \phi_3^2)^{1/2}$ is the rotational norm or the length of the rotational vector. An expansion of trigonometric functions in Eq. (8) in MacLaurin's series yields

$$\boldsymbol{R} = \boldsymbol{I} + \boldsymbol{S} + \frac{1}{2!}\boldsymbol{S}^2 + \frac{1}{3!}\boldsymbol{S}^3 + \cdots + \frac{1}{n!}\boldsymbol{S}^n + \cdots = \exp\boldsymbol{S}. \tag{9}$$

Thus, the rotation matrix may alternatively be expressed by an exponential map, the exponentiation of the spin matrix associated with the rotational vector. Note that, as a consequence of the exponentiation of the spin matrix $\boldsymbol{S}(\boldsymbol{\phi})$ being equal to $\boldsymbol{R}(\boldsymbol{\phi}) \in$ SO(3), the spin matrix $\boldsymbol{S}(\boldsymbol{\phi})$ belongs to Lie algebra so(3) associated with the Lie group SO(3) [28].

Conversely, taking a given orthogonal matrix $\boldsymbol{R}$ as a rotation matrix, the associated rotation vector $\boldsymbol{\phi}$ can be derived from (7) and (8). The rotational norm ϕ can be calculated by

$$\phi = \cos^{-1}\frac{Tr(\boldsymbol{R}) - 1}{2}. \tag{10}$$

By taking the matrix logarithm of $\boldsymbol{R}$ we can obtain the skew-symmetric matrix $\boldsymbol{S}$ as following.

$$\boldsymbol{S} = \log \boldsymbol{R} = \frac{\phi}{2\sin\phi}(\boldsymbol{R} - \boldsymbol{R}^T). \tag{11}$$

Therefore $\boldsymbol{\phi} = \phi_i \mathbf{e}_i$ with $\phi_1 = -S_{23}$, $\phi_2 = S_{13}$, and $\phi_3 = -S_{12}$.

In terms of the rotational vector $\boldsymbol{\phi}$, Eqs. (7) and (8) give the exact value of the current rotation matrix. Using truncated MacLaurin's series of various order in Eq. (9), approximate values of the rotation matrix are obtained and corresponding simplified theories can be derived. For example, a so called first order theory is obtained if small rotations are assumed so that the quadratic and higher order terms in Eq. (9) may be neglected.

2.3 Specifications for the deformed configuration space

The position vector $\mathbf{r}(s,t)$ defined by (1) is an element of Euclidean vector space $\mathscr{R}^3$. The orientation of the moving basis is represented by the rotation matrix, which is en element of the Lie group SO(3). Accordingly, the set of all possible configurations of the rod is defined by

$$\mathscr{C} = \{(\mathbf{r}, \boldsymbol{R}) |\, \mathbf{r} : s \to \mathscr{R}^3,\ \boldsymbol{R} : s \to \mathrm{SO}(3)\}. \tag{12}$$

This set is referred to as the deformed configuration space. The quantities $\mathbf{r}$ and $\boldsymbol{R}$ are termed the kinematic quantities of the rod. Since the rotation matrix is related to the three parameters, the components of the rotational vector $\boldsymbol{\phi}$, the Lie group SO(3) of rotation matrices is three-parametric, i.e. it may be viewed as being a 3-D nonlinear differentiable manifold.

For a typical slender rod such as the components in MEMS, the effect of shearing deformation can be negligible, the cross-section of the rod is therefore assumed to be perpendicular to the tangent to the Cosserat curve, i.e.

$$\mathbf{v}(s,t) = \partial_s \mathbf{r}(s,t) = |\partial_s \mathbf{r}(s,t)|\, \mathbf{d}_3(s,t). \tag{13}$$

In this case, we write

$$\mathbf{d}_3(s,t) = \frac{\partial_s \mathbf{r}(s,t)}{|\partial_s \mathbf{r}(s,t)|} \triangleq \nu_1(s,t)\mathbf{e}_1 + \nu_2(s,t)\mathbf{e}_2 + \nu_3(s,t)\mathbf{e}_3 \tag{14}$$

with

$$\nu_1^2(s,t) + \nu_2^2(s,t) + \nu_3^2(s,t) = 1. \tag{15}$$

where ν_1, ν_2 and ν_3 can be written as

$$\nu_1(s,t) = \frac{\partial_s x(s,t)}{|\partial_s \mathbf{r}(s,t)|}, \quad \nu_2(s,t) = \frac{\partial_s y(s,t)}{|\partial_s \mathbf{r}(s,t)|}, \quad \text{and} \quad \nu_3(s,t) = \frac{\partial_s z(s,t)}{|\partial_s \mathbf{r}(s,t)|}, \tag{16}$$

by differentiating the position vector $\mathbf{r}(s,t)$ defined in (1) with respect to s.

We assume that the directors $\{\mathbf{d}_1, \mathbf{d}_2, \mathbf{d}_3\}$ can be obtained by the following way. First of all, we rotate directors $\{\mathbf{e}_1, \mathbf{e}_2, \mathbf{e}_3\}$ about $\mathbf{e}_3$ with an angle φ to obtain the directors $\{\tilde{\mathbf{d}}_1, \tilde{\mathbf{d}}_2, \mathbf{e}_3\}$. Then, rotation matrix $\boldsymbol{R}_a$ associated with the rotational vector $\boldsymbol{\phi_a} = \varphi\, \mathbf{e}_3$ can be written as

$$\boldsymbol{R}_a = \boldsymbol{R}(\boldsymbol{\phi_a}) = \begin{bmatrix} \cos\varphi & -\sin\varphi & 0 \\ \sin\varphi & \cos\varphi & 0 \\ 0 & 0 & 1 \end{bmatrix}. \tag{17}$$

Next, we introduce a rotational vector

$$\boldsymbol{\phi_b} = -\frac{\sin^{-1}\sqrt{\nu_1^2+\nu_2^2}}{\sqrt{\nu_1^2+\nu_2^2}}\,\nu_2\,\tilde{\mathbf{d}}_1 + \frac{\sin^{-1}\sqrt{\nu_1^2+\nu_2^2}}{\sqrt{\nu_1^2+\nu_2^2}}\,\nu_1\,\tilde{\mathbf{d}}_2$$

which rotates the vectors $\{\tilde{\mathbf{d}}_1, \tilde{\mathbf{d}}_2, \mathbf{e}_3\}$ to $\{\mathbf{d}_1, \mathbf{d}_2, \mathbf{d}_3\}$. Here, we assume that $\nu_1^2 + \nu_2^2 \neq 0$. Other wise $\mathbf{d}_3 = \mathbf{e}_3$, this rotating procedure can be omitted. Let $\boldsymbol{R}_b$ be the corresponding rotation matrix associated with the rotational vector $\boldsymbol{\phi_b}$. Then

$$\boldsymbol{R}_b = \boldsymbol{R}(\boldsymbol{\phi_b}) = \begin{bmatrix} \frac{\nu_1^2\nu_3+\nu_2^2}{\nu_1^2+\nu_2^2} & \frac{\nu_1\nu_2(\nu_3-1)}{\nu_1^2+\nu_2^2} & \nu_1 \\ \frac{\nu_1\nu_2(\nu_3-1)}{\nu_1^2+\nu_2^2} & \frac{\nu_2^2\nu_3+\nu_1^2}{\nu_1^2+\nu_2^2} & \nu_2 \\ -\nu_1 & \nu_2 & \nu_3 \end{bmatrix}. \tag{18}$$

Consequently, the moving directors are obtained as:

$$\begin{aligned} \mathbf{d}_1 =& \left(\frac{(\nu_1^2\nu_3+\nu_2^2)\cos\varphi}{\nu_1^2+\nu_2^2} + \frac{\nu_1\nu_2(\nu_3-1)\sin\varphi}{\nu_1^2+\nu_2^2}\right)\mathbf{e}_1 \\ &+ \left(\frac{(\nu_2^2\nu_3+\nu_1^2)\sin\varphi}{\nu_1^2+\nu_2^2} + \frac{\nu_1\nu_2(\nu_3-1)\cos\varphi}{\nu_1^2+\nu_2^2}\right)\mathbf{e}_2 - (\nu_1\cos\varphi + \nu_2\sin\varphi)\,\mathbf{e}_3, \end{aligned} \tag{19}$$

$$\begin{aligned} \mathbf{d}_2 =& \left(-\frac{(\nu_1^2\nu_3+\nu_2^2)\sin\varphi}{\nu_1^2+\nu_2^2} + \frac{\nu_1\nu_2(\nu_3-1)\cos\varphi}{\nu_1^2+\nu_2^2}\right)\mathbf{e}_1 \\ &+ \left(\frac{(\nu_2^2\nu_3+\nu_1^2)\cos\varphi}{\nu_1^2+\nu_2^2} - \frac{\nu_1\nu_2(\nu_3-1)\sin\varphi}{\nu_1^2+\nu_2^2}\right)\mathbf{e}_2 + (\nu_1\sin\varphi - \nu_2\cos\varphi)\,\mathbf{e}_3, \end{aligned} \tag{20}$$

$$\mathbf{d}_3 = \nu_1\mathbf{e}_1 + \nu_2\mathbf{e}_2 + \nu_3\mathbf{e}_3. \tag{21}$$

Obviously $\varphi(s,t)$ is a variable related to torsion of the rod. Expanding the directors in polynomials about ν_1, ν_2, ϕ and reserving the terms up to third order, we have

$$\begin{aligned}
\mathbf{d}_1(s,t) \approx & \left(1-\frac{1}{2}\varphi^2(s,t)-\frac{1}{2}\nu_1^2(s,t)-\frac{1}{2}\nu_1(s,t)\nu_2(s,t)\varphi(s,t)\right)\mathbf{e}_1 \\
& +\left(\varphi(s,t)-\frac{1}{2}\nu_1(s,t)\nu_2(s,t)-\frac{1}{2}\nu_2^2(s,t)\varphi(s,t)-\frac{1}{6}\varphi^3(s,t)\right)\mathbf{e}_2 \\
& +\left(-\nu_1(s,t)-\nu_2(s,t)\varphi(s,t)+\frac{1}{2}\nu_1(s,t)\varphi^2(s,t)\right)\mathbf{e}_3 \qquad (22)\\
\mathbf{d}_2(s,t) \approx & \left(-\varphi(s,t)-\frac{1}{2}\nu_1(s,t)\nu_2(s,t)+\frac{1}{2}\nu_1^2(s,t)\varphi(s,t)+\frac{1}{6}\phi^3(s,t)\right)\mathbf{e}_1 \\
& +\left(1-\frac{1}{2}\varphi^2(s,t)-\frac{1}{2}\nu_2^2(s,t)+\frac{1}{2}\nu_1(s,t)\nu_2(s,t)\varphi(s,t)\right)\mathbf{e}_2 \\
& +\left(-\nu_2(s,t)+\nu_1(s,t)\phi(s,t)+\frac{1}{2}\nu_2(s,t)\varphi^2(s,t)\right)\mathbf{e}_3 \qquad (23)\\
\mathbf{d}_3(s,t) \approx & \nu_1(s,t)\mathbf{e}_1+\nu_2(s,t)\mathbf{e}_2+\left(1-\frac{1}{2}\nu_1^2(s,t)-\frac{1}{2}\nu_2^2(s,t)\right)\mathbf{e}_3 \qquad (24)
\end{aligned}$$

For the sake of convenience to describe the displacements and rotations in the inertia frame, we regard directors $\mathbf{d}_i(s,t)$ $(i=1,2,3)$ as those obtained by rotating inertial frame $\{\mathbf{e}_1,\mathbf{e}_2,\mathbf{e}_3\}$ with a rotation vector

$$\boldsymbol{\phi}=\phi_x(s,t)\mathbf{e}_1+\phi_y(s,t)\mathbf{e}_2+\phi_z(s,t)\mathbf{e}_3. \qquad (25)$$

Now, based on the relations (19)–(21), utilizing the inverse procedure mentioned in Section 2.2, the rotational norm ϕ and the spin matrix associated with the rotation vector $\boldsymbol{\phi}$ in (25) can be derived from

$$\phi=\cos^{-1}\frac{Tr(\boldsymbol{R}_b\boldsymbol{R}_a)-1}{2}. \qquad (26)$$

and

$$\boldsymbol{S}=\log(\boldsymbol{R}_b\boldsymbol{R}_a)=\frac{\phi}{2\sin\phi}(\boldsymbol{R}_b\boldsymbol{R}_a-\boldsymbol{R}_a^T\boldsymbol{R}_b^T). \qquad (27)$$

Consequently, the approximate relations between (ϕ_x,ϕ_y,ϕ_z) and (ν_1,ν_2,φ), up to third order, are obtained as

$$\begin{cases}
\phi_x(s,t)=-\nu_2(s,t)+\dfrac{1}{2}\,\varphi(s,t)\nu_1(s,t)-\dfrac{1}{6}\,\left(\nu_1^2(s,t)+\nu_2^2(s,t)-\dfrac{1}{2}\,\varphi^2(s,t)\right)\nu_2(s,t), \\
\phi_y(s,t)=\nu_1(s,t)+\dfrac{1}{2}\,\varphi(s,t)\nu_2(s,t)+\dfrac{1}{6}\,\left(\nu_1^2(s,t)+\nu_2^2(s,t)-\dfrac{1}{2}\,\varphi^2(s,t)\right)\nu_1(s,t), \\
\phi_z(s,t)=\varphi(s,t)-\dfrac{1}{12}\,\left(\nu_1^2(s,t)+\nu_2^2(s,t)\right)\varphi(s,t),
\end{cases} \qquad (28)$$

or equivalently,

$$\begin{cases} \nu_1(s,t) = \phi_y(s,t) + \dfrac{1}{2}\,\phi_x(s,t)\phi_z(s,t) - \dfrac{1}{6}\,\left(\phi_x^2(s,t) + \phi_y^2(s,t) + \phi_z^3(s,t)\right)\phi_y(s,t), \\ \nu_2(s,t) = -\phi_x(s,t) + \dfrac{1}{2}\,\phi_y(s,t)\phi_z(s,t) + \dfrac{1}{6}\,\left(\phi_x^2(s,t) + \phi_y^2(s,t) + \phi_z^2(s,t)\right)\phi_x(s,t), \\ \varphi(s,t) = \phi_z(s,t) + \dfrac{1}{12}\,\left(\phi_x^2(s,t) + \phi_y^2(s,t)\right)\phi_z(s,t). \end{cases} \tag{29}$$

These relations are very useful in solving the static problem and will be used below to derive the shape functions for CRD.

3 The Governing Equations of Motion

The dynamical evolution of the rod with density, $\rho(s)$, and cross-section area, $A(s)$ is governed by the Newton's dynamical laws:

$$\begin{cases} \rho(s)A(s)\partial_{tt}\mathbf{r} = \partial_s\mathbf{n}(s,t) + \mathbf{f}(s,t), \\ \partial_t\mathbf{h}(s,t) = \partial_s\mathbf{m}(s,t) + \mathbf{v}(s,t)\times\mathbf{n}(s,t) + \mathbf{l}(s,t), \end{cases} \tag{30}$$

where

$$\mathbf{n}(s,t) = n_i(s,t)\mathbf{d}_i(s,t), \quad \mathbf{m}(s,t) = m_i(s,t)\mathbf{d}_i(s,t) \tag{31}$$

are the contact force and contact torque densities, respectively; while

$$\mathbf{h}(s,t) = h_i(s,t)\mathbf{d}_i(s,t) \tag{32}$$

denotes the angular momentum densities; $\mathbf{f}(s,t)$ and $\mathbf{l}(s,t)$ denote the prescribed external force and torque densities, respectively.

The simplest constitutive model is based on the Kirchoff constitutive relations which provide an adequate description of elastic properties in terms of a few elastic moduli. One may exploit the full versatility of the Cosserat model by generating the Kirchoff constitutive relations to include viscoelasticity and other damping, curved reference states with memory and effects to prohibit total compression.

The contact forces, contact torques and the angular momentum are given as

$$\mathbf{n} = \mathbf{K}(\mathbf{v} - \mathbf{d}_3), \qquad \mathbf{m} = \mathbf{J}(\mathbf{u}), \qquad \mathbf{h} = \mathbf{I}(\mathbf{w}) \tag{33}$$

where, according to the Kirchoff constitutive relations, the tensors $\mathbf{K}$, $\mathbf{J}$ and $\mathbf{I}$ are described as

$$\begin{cases} \mathbf{K}(s,t) = K_{ii}(s,t)(\mathbf{d}_i(s,t) \otimes \mathbf{d}_i(s,t)), \\ \mathbf{J}(s,t) = \sum_{i,j=1}^{2} J_{ij}(s,t)(\mathbf{d}_i(s,t) \otimes \mathbf{d}_j(s,t)) + J_{33}(s,t)(\mathbf{d}_3(s,t) \otimes \mathbf{d}_3(s,t)), \\ \mathbf{I}(s,t) = \sum_{i,j=1}^{2} I_{ij}(s,t)(\mathbf{d}_i(s,t) \otimes \mathbf{d}_j(s,t)) + I_{33}(s,t)(\mathbf{d}_3(s,t) \otimes \mathbf{d}_3(s,t)). \end{cases} \tag{34}$$

The corresponding components are given as

$$\begin{cases} K_{11} = K_{22} = GA(s), & K_{33} = EA(s), \\ J_{11} = \int_{A(s)} E\eta^2 \, dA, & J_{22} = \int_{A(s)} E\xi^2 \, dA, \\ J_{33} = \int_{A(s)} G(\xi^2 + \eta^2) \, dA, & J_{12} = -J_{21} = \int_{A(s)} E\xi\eta \, dA, \\ I_{11} = \int_{A(s)} \rho(s)\eta^2 \, dA, & I_{22} = \int_{A(s)} \rho(s)\xi^2 \, dA, \\ I_{33} = \int_{A(s)} \rho(s)(\xi^2 + \eta^2) \, dA, & I_{12} = -I_{21} = \int_{A(s)} \rho(s)\xi\eta \, dA, \end{cases} \tag{35}$$

where E and G are the Young's modulus of elasticity and shear modulus respectively.

4 Shape Functions for Cosserat Rod Elements

For convenience, consider a uniform and initially straight rod element of constant length L, supported in an arbitrary manner at $s = a = 0$ and $s = b = L$. It is assumed in the following that the static equilibrium of the rod corresponds to the situation where the directions of $\mathbf{d}_3$ and $\mathbf{e}_3$ are coincident with each other and $\mathbf{d}_1$, $\mathbf{d}_2$ are parallel to $\mathbf{e}_1$, $\mathbf{e}_2$, respectively. The principal axes are chosen to parallel $\mathbf{e}_1$, $\mathbf{e}_2$ and $\mathbf{e}_3$. For the sake of simplicity, it will be assumed that the axes along the directors $\mathbf{d}_1$, $\mathbf{d}_2$ and $\mathbf{d}_3$ are chosen to be the principal axes of inertia of the cross section at s, and centered at the cross section's center of mass. Then, for a uniform rod with cross-section area $A(s)$, we have $J_{12} = J_{21} = 0$, $I_{12} = I_{21} = 0$ and

$$\begin{cases} K_{11} = K_{22} = GA(s), & K_{33} = EA(s), \\ J_{11} = E\int_{A(s)} \eta^2 \, dA, & J_{22} = E\int_{A(s)} \xi^2 \, dA, \\ I_{11} = \rho\int_{A(s)} \eta^2 \, dA, & I_{22} = \rho\int_{A(s)} \xi^2 \, dA, \\ J_{33} = G\int_{A(s)} (\xi^2 + \eta^2) \, dA = \frac{G}{E}(J_{11} + J_{22}), & \\ I_{33} = \rho\int_{A(s)} (\xi^2 + \eta^2) \, dA = I_{11} + I_{22}. & \end{cases} \tag{36}$$

Assume that the shape functions for a CRE satisfy the corresponding static equations of (30), i.e.

$$\partial_s \mathbf{n}(s) = 0 \tag{37}$$

$$\partial_s \mathbf{m}(s) + \mathbf{v}(s) \times \mathbf{n}(s) = 0, \tag{38}$$

where the contact force and contact torque densities are

$$\begin{cases} \mathbf{n}(s) = n_i(s)\mathbf{d}_i(s), \quad n_1 = K_{11}v_1, \quad n_2 = K_{22}v_2, \quad n_3 = K_{33}(v_3 - 1), \\ \mathbf{m}(s) = m_i(s)\mathbf{d}_i(s), \quad m_1 = J_{11}u_1, \quad m_2 = J_{22}u_2, \quad m_3 = J_{33}u_3. \end{cases} \tag{39}$$

with $\mathbf{u}(s) = \frac{1}{2}\mathbf{d}_i(s) \times \partial_s \mathbf{d}_i(s)$, and $\mathbf{d}_i(s)$ $(i = 1, 2, 3)$ are given by (22)–(24).

As mentioned in Section 2.3, for a typical slender rod as the components in MEMS, the effect of shearing deformation can be negligible, therefore the cross-section of rod is assumed to be perpendicular to the tangent to the Cosserat curve, i.e. the strain vector $\mathbf{v}(s,t) = |\partial_s \mathbf{r}(s)|\, \mathbf{d}_3(s)$ satisfies the form (13). Thus, $v_1 = v_2 = 0$ and $v_3 = |\partial_s \mathbf{r}(s)|$. Consequently, instead of $n_1 = K_{11}v_1$ and $n_2 = K_{22}v_2$, the contact forces n_1 and n_2 follow from (38)

$$n_1 = \frac{-\partial_s m_2 - u_3 m_1 + u_1 m_3}{v_3}, \quad \text{and} \quad n_2 = \frac{\partial_s m_1 - u_3 m_2 + u_2 m_3}{v_3}. \tag{40}$$

As a prelude to expanding the nonlinear shape functions to a form suitable for a perturbation analysis of the motion, it is useful to introduce some natural scales to obtain a dimensionless equation of motion. Introduce the dimensionless variables

$$\sigma = \frac{s}{L_0},\ \bar{\mathbf{r}} = \frac{\mathbf{r}}{L_0},\ \bar{x} = \frac{x}{L_0},\ \bar{y} = \frac{y}{L_0},\ \bar{z} = \frac{z}{L_0},\ \tau = \omega_0 t, \tag{41}$$

where L_0 and ω_0 are the reference length and natural frequency yet to be determined later, respectively.

Assume that the dimensionless generic nodal displacements (boundary displacements and rotations) at $\sigma = 0$ and $\sigma = L/L_0$ are

$$\boldsymbol{q}_a = \Big[\, \epsilon X_a \ \epsilon Y_a \ \epsilon Z_a \ \epsilon \Phi_{xa} \ \epsilon \Phi_{ya} \ \epsilon \Phi_{za} \,\Big]^T \tag{42}$$

and

$$\boldsymbol{q}_b = \Big[\, \epsilon X_b \ \epsilon Y_b \ \epsilon Z_b \ \epsilon \Phi_{xb} \ \epsilon \Phi_{yb} \ \epsilon \Phi_{zb} \,\Big]^T, \tag{43}$$

respectively. Substituting (42) and (43) into (1), we obtain the boundary conditions for $\bar{x}$, $\bar{y}$ and $\bar{z}$ as

$$\begin{cases} \bar{x}(0) = \epsilon X_a, \quad \bar{y}(0) = \epsilon Y_a, \quad \bar{z}(0) = \epsilon Z_a, \\ \bar{x}(l) = \epsilon X_b, \quad \bar{y}(l) = \epsilon Y_b, \quad \bar{z}(l) = l + \epsilon Z_b, \end{cases} \tag{44}$$

where $l = L/L_0$ is the dimensionless length of the rod element. Substituting (42) and (43) into (29), we

obtain the boundary conditions for ν_1, ν_2 and φ as

$$\begin{cases} \nu_1(0) = \dfrac{\bar{x}'(0)}{|\bar{\mathbf{r}}'(0)|} = \epsilon\Phi_{ya} + \dfrac{1}{2}\epsilon^2\Phi_{xa}\Phi_{za} - \dfrac{1}{6}\epsilon^3\left(\Phi_{xa}^2 + \Phi_{ya}^2 + \Phi_{za}^2\right)\Phi_{ya}, \\ \nu_2(0) = \dfrac{\bar{y}'(0)}{|\bar{\mathbf{r}}'(0)|} = -\epsilon\Phi_{xa} + \dfrac{1}{2}\epsilon^2\Phi_{ya}\Phi_{za} + \dfrac{1}{6}\epsilon^3\left(\Phi_{xa}^2 + \Phi_{ya}^2 + \Phi_{za}^2\right)\Phi_{xa}, \\ \varphi(0) = \epsilon\Phi_{za} + \dfrac{1}{12}\epsilon^3\left(\Phi_{xa}^2 + \Phi_{ya}^2\right)\Phi_{za} \\ \nu_1(l) = \dfrac{\bar{x}'(l)}{|\bar{\mathbf{r}}'(l)|} = \epsilon\Phi_{yb} + \dfrac{1}{2}\epsilon^2\Phi_{xb}\Phi_{zb} - \dfrac{1}{6}\epsilon^3\left(\Phi_{xb}^2 + \Phi_{yb}^2 + \Phi_{zb}^2\right)\Phi_{yb}, \\ \nu_2(l) = \dfrac{\bar{y}'(l)}{|\bar{\mathbf{r}}'(l)|} = -\epsilon\Phi_{xb} + \dfrac{1}{2}\epsilon^2\Phi_{yb}\Phi_{zb} + \dfrac{1}{6}\epsilon^3\left(\Phi_{xb}^2 + \Phi_{yb}^2 + \Phi_{zb}^2\right)\Phi_{xb}, \\ \varphi(l) = \epsilon\Phi_{zb} + \dfrac{1}{12}\epsilon^3\left(\Phi_{xb}^2 + \Phi_{yb}^2\right)\Phi_{zb} \end{cases} \tag{45}$$

Treating ϵ as a perturbation parameter which is the order of the amplitude of the displacement and can be used as a crutch in obtaining the approximate solution, the shape functions can be obtained by solving the static equations (37) and (38) with the corresponding boundary conditions (44) and (45) and also the restrictions (40) on the assumption of neglecting the effect of shearing deformation. To do this, we seek a straightforward expansion

$$\begin{cases} \bar{x}(\sigma) = \epsilon\hat{x}_1(\sigma) + \epsilon^2\hat{x}_2(\sigma) + \epsilon^3\hat{x}_3(\sigma) + \cdots, \\ \bar{y}(\sigma) = \epsilon\hat{y}_1(\sigma) + \epsilon^2\hat{y}_2(\sigma) + \epsilon^3\hat{y}_3(\sigma) + \cdots, \\ \bar{z}(\sigma) = \sigma + \epsilon\hat{z}_1(\sigma) + \epsilon^2\hat{z}_2(\sigma) + \epsilon^3\hat{z}_3(\sigma) + \cdots, \\ \varphi(\sigma) = \epsilon\hat{\varphi}_1(\sigma) + \epsilon^2\hat{\varphi}_2(\sigma) + \epsilon^3\hat{\varphi}_3(\sigma) + \cdots. \end{cases} \tag{46}$$

Substituting (46) into (37) and (38) associated with (40) and, because $\bar{x}_i$, $\bar{y}_i$, $\bar{z}_i$ and $\bar{\varphi}_i$ are independent of ϵ, set the coefficient of each power of ϵ equal to zero. This leads to a set of linear ordinary differential equations which can be solved using the Frobeniu's method [29] under the corresponding boundary conditions (44) and (45). The solving procedure has been implemented in a MAPLE file [30]. Consequently, the approximate series solutions are obtained and the 1st order ones are

$$\begin{cases} \hat{x}_1(\sigma) = X_a & + \Phi_{ya}\sigma - (3X_a - 3X_b + 2l\Phi_{ya} + l\Phi_{yb})\dfrac{\sigma^2}{l^2} \\ & \quad + (2X_a - 2X_b + l\Phi_{ya} + l\Phi_{yb})\dfrac{\sigma^3}{l^3} \\ \hat{y}_1(\sigma) = Y_a & - \Phi_{xa}\sigma - (3Y_a - 3Y_b - 2l\Phi_{xa} - l\Phi_{xb})\dfrac{\sigma^2}{l^2} \\ & \quad + (2Y_a - 2Y_b - l\Phi_{xa} - l\Phi_{xb})\dfrac{\sigma^3}{l^3} \\ \hat{z}_1(\sigma) = Z_a & + (Z_b - Z_a)\dfrac{\sigma}{l} \\ \hat{\varphi}_1(\sigma) = \Phi_{za} & + (\Phi_{zb} - \Phi_{za})\dfrac{\sigma}{l}. \end{cases} \tag{47}$$

To investigate deflections up to 3rd order nonlinearity in ϵ it is adequate to adopt the truncated (46) to ϵ^3 order terms. The high order terms (up to third order) which are polynomials of σ, can be easily solved using a MAPLE programm [30]. For example, $\hat{x}_2(\sigma) = C_1\sigma^5 + C_2\sigma^4 + C_3\sigma^3 + C_4\sigma^2$ with

$$C_1 = \frac{K_{33}}{20l^4 J_{22}}(Z_b - Z_a)(2X_a - 2X_b + l\Phi_{ya} + l\Phi_{yb}). \tag{48}$$

Accordingly to the time-dependent, rod shape under the quasi-static condition is specified with the (slowly) time-varying nodal displacements and rotations.

5 Equations of Motion for Cosserat Rod Elements

In this section, the Lagrangian approach is employed to formulate the ordinary differential equations of motion of Cosserat rod elements. The generalized Hamilton's principle which, in its most general form, is given by the variational statement

$$\int_{t_1}^{t_2} \delta(\mathscr{T} - \mathscr{V})dt + \int_{t_1}^{t_2} \delta\mathscr{W}\, dt = 0, \tag{49}$$

where $\mathscr{T}$ is the total kinetic energy of the system, $\mathscr{V}$ is the potential energy of the system (including the strain energy and the potential energy of conservative external forces), $\delta(\,\cdot\,)$ represents the virtual displacement (or variational) operator, and $\delta\mathscr{W}$ is the virtual work done by nonconservative forces (including damping forces) and external forces not accounted for in $\mathscr{V}$.

Assume that the time-varying dimensionless displacements at the ends ($\sigma = a/L_0$ and $\sigma = b/L_0$) of the element model are

$$\boldsymbol{q}_a(\tau) = \Big[\, X_a(\tau)\ Y_a(\tau)\ Z_a(\tau)\ \Phi_{xa}(\tau)\ \Phi_{ya}(\tau)\ \Phi_{za}(\tau) \,\Big]^T \tag{50}$$

and

$$\boldsymbol{q}_b(\tau) = \Big[\, X_b(\tau)\ Y_b(\tau)\ Z_b(\tau)\ \Phi_{xb}(\tau)\ \Phi_{yb}(\tau)\ \Phi_{zb}(\tau) \,\Big]^T, \tag{51}$$

respectively. Then, the generalized displacement vector for the element can be described by

$$\boldsymbol{q}^e(\tau) = \Big[\, \boldsymbol{q}_a^T(\tau)\ \boldsymbol{q}_b^T(\tau) \,\Big]^T \tag{52}$$

Consistent with the kinematic and constitutive assumptions described in Section 2 and Section 3 and the shape functions derived in Section 4, the kinetic energy per unit length is

$$\mathcal{T} = \frac{1}{2}\left\{\rho A\, \partial_t \mathbf{r} \cdot \partial_t \mathbf{r} + \mathbf{I}(\mathbf{w}, \mathbf{w})\right\} = \frac{1}{2}\left\{\rho A \omega_0^2 L_0^2\, \dot{\bar{\mathbf{r}}} \cdot \dot{\bar{\mathbf{r}}} + \omega_0^2 \mathbf{I}(\bar{\mathbf{w}}, \bar{\mathbf{w}})\right\} \tag{53}$$

where ρ and A are the density of rod and the area of cross-section of rod, respectively. According to (1) and (4), the velocity $\partial_t \mathbf{r}(s,t)$, and the angular velocity of the cross-section can be derived as:

$$\partial_t \mathbf{r} = \partial_t x \mathbf{e}_1 + \partial_t y \mathbf{e}_2 + \partial_t z \mathbf{e}_3 = \omega_0 L_0 (\dot{\bar{x}} \mathbf{e}_1 + \dot{\bar{y}} \mathbf{e}_2 + \dot{\bar{z}} \mathbf{e}_3) = \omega_0 L_0 \dot{\bar{\mathbf{r}}} \tag{54}$$

and

$$\mathbf{w} = \frac{1}{2} \mathbf{d}_i \times \partial_t \mathbf{d}_i = \frac{1}{2} \omega_0 \mathbf{d}_i \times \dot{\mathbf{d}}_i = \omega_0 \bar{\mathbf{w}}, \tag{55}$$

respectively.

Under small strain conditions the strain energy per unit length of rod can be expressed in terms of the strain vectors $\mathbf{u}$ and $\mathbf{v}$ as:

$$\mathcal{U} = \frac{1}{2} \left\{ \mathbf{J}(\mathbf{u}, \mathbf{u}) + K_{33} (v_3 - 1)^2 \right\} = \frac{1}{2} \left\{ \frac{1}{L_0^2} \mathbf{J}(\bar{\mathbf{u}}, \bar{\mathbf{u}}) + K_{33} (\bar{v}_3 - 1)^2 \right\} \tag{56}$$

where the strain vector is

$$\mathbf{u} = \frac{1}{2} \mathbf{d}_i \times \partial_s \mathbf{d}_i = \frac{1}{2L_0} \mathbf{d}_i \times \mathbf{d}_i' = \frac{1}{L_0} \bar{\mathbf{u}} \quad \text{and} \quad v_3 = |\partial_s \mathbf{r}| = |\mathbf{r}'| = \bar{v}_3. \tag{57}$$

Utilizing the time varying generic nodal displacements introduced in (50) and (51) instead of the static generic nodal displacements introduced in (42) and (43) respectively, the time varying generic displacements at any point within the element can be expressed as nonlinear functions of the length parameter σ and the nodal displacement vector $\boldsymbol{q}^e(\tau)$. Based on the nonlinear shape functions derived in Section 4, we have

$$\begin{cases} \bar{x} = \hat{x}_1(\sigma,\tau) + \hat{x}_2(\sigma,\tau) + \hat{x}_3(\sigma,\tau), \\ \bar{y} = \hat{y}_1(\sigma,\tau) + \hat{y}_2(\sigma,\tau) + \hat{y}_3(\sigma,\tau), \\ \bar{z} = \sigma + \hat{z}_1(\sigma,\tau) + \hat{z}_2(\sigma,\tau) + \hat{z}_3(\sigma,\tau), \\ \varphi = \hat{\varphi}_1(\sigma,\tau) + \hat{\varphi}_2(\sigma,\tau) + \hat{\varphi}_3(\sigma,\tau). \end{cases} \tag{58}$$

where the ith terms $\hat{x}_i$, $\hat{y}_i$, $\hat{z}_i$ and $\hat{\varphi}_i$ are ith order functions of the nodal displacement vector $\boldsymbol{q}^e(\tau)$. For example, based on (47) the 1st order terms are

$$\begin{cases} \hat{x}_1(\sigma,\tau) = X_a(\tau) & + \Phi_{ya}(\tau)\sigma - (3X_a(\tau) - 3X_b(\tau) + 2l\Phi_{ya}(\tau) + l\Phi_{yb}(\tau))\dfrac{\sigma^2}{l^2} \\ & + (2X_a(\tau) - 2X_b(\tau) + l\Phi_{ya}(\tau) + l\Phi_{yb}(\tau))\dfrac{\sigma^3}{l^3} \\ \hat{y}_1(\sigma,\tau) = Y_a(\tau) & - \Phi_{xa}(\tau)\sigma - (3Y_a(\tau) - 3Y_b(\tau) - 2l\Phi_{xa}(\tau) - l\Phi_{xb}(\tau))\dfrac{\sigma^2}{l^2} \\ & + (2Y_a(\tau) - 2Y_b(\tau) - l\Phi_{xa}(\tau) - l\Phi_{xb}(\tau))\dfrac{\sigma^3}{l^3} \\ \hat{z}_1(\sigma,\tau) = Z_a(\tau) & + (Z_b(\tau) - Z_a(\tau))\dfrac{\sigma}{l} \\ \hat{\phi}_1(\sigma,\tau) = \Phi_{za}(\tau) & + (\Phi_{zb}(\tau) - \Phi_{za}(\tau))\dfrac{\sigma}{l}. \end{cases} \tag{59}$$

The high order terms (up to third order), as indicated in Section 4, can be easily obtained using a MAPLE program [30]. Consequently, the time varying generic displacements at any point within the element can be written as

$$\bar{x} = \bar{x}(\sigma, \boldsymbol{q}^e(\tau)), \quad \bar{y} = \bar{y}(\sigma, \boldsymbol{q}^e(\tau)), \quad \bar{z} = \bar{z}(\sigma, \boldsymbol{q}^e(\tau)), \quad \varphi = \varphi(\sigma, \boldsymbol{q}^e(\tau)). \tag{60}$$

This leads $\bar{\mathbf{r}} = \bar{\mathbf{r}}(\sigma, \boldsymbol{q}^e(\tau))$. Moreover, from (16), we have

$$\nu_1 = \frac{\bar{x}'(\sigma, \boldsymbol{q}^e(\tau))}{|\bar{\mathbf{r}}'(\sigma, \boldsymbol{q}^e(\tau))|} = \nu_1(\sigma, \boldsymbol{q}^e(\tau)), \quad \nu_2 = \frac{\bar{y}'(\sigma, \boldsymbol{q}^e(\tau))}{|\bar{\mathbf{r}}'(\sigma, \boldsymbol{q}^e(\tau))|} = \nu_2(\sigma, \boldsymbol{q}^e(\tau)) \tag{61}$$

Substituting $\nu_1(\sigma, \boldsymbol{q}^e(\tau))$, $\nu_2(\sigma, \boldsymbol{q}^e(\tau))$ and $\varphi(\sigma, \boldsymbol{q}^e(\tau))$ into the expressions (22)–(24) yields

$$\mathbf{d}_i = \mathbf{d}_i(\sigma, \boldsymbol{q}^e(\tau)), \qquad i = 1, 2, 3. \tag{62}$$

Similarly, from (28), we have

$$\phi_x = \phi_x(\sigma, \boldsymbol{q}^e(\tau)), \quad \phi_y = \phi_y(\sigma, \boldsymbol{q}^e(\tau)), \quad \phi_z = \phi_z(\sigma, \boldsymbol{q}^e(\tau)). \tag{63}$$

It follows from (55), (57) and (62) that

$$\bar{\mathbf{w}} = \frac{1}{2}\mathbf{d}_i \times \dot{\mathbf{d}}_i = \bar{\mathbf{w}}(\sigma, \boldsymbol{q}^e(\tau)), \quad \bar{\mathbf{u}} = \frac{1}{2}\mathbf{d}_i \times \mathbf{d}_i' = \bar{\mathbf{u}}(\sigma, \boldsymbol{q}^e(\tau)) \tag{64}$$

Therefore, the kinetic energy density (53) and the potential energy density (56) are expressed as

$$\mathcal{T} = \mathcal{T}(\sigma, \boldsymbol{q}^e(\tau), \dot{\boldsymbol{q}}^e(\tau)), \quad \mathcal{U} = \mathcal{U}(\sigma, \boldsymbol{q}^e(\tau)). \tag{65}$$

Then, the Lagrangian defined in the classical form $\mathscr{L} = \mathscr{T} - \mathscr{V}$ are obtained as

$$\mathscr{L}(\boldsymbol{q}^e, \dot{\boldsymbol{q}}^e) = \mathscr{T}(\boldsymbol{q}^e, \dot{\boldsymbol{q}}^e) - \mathscr{V}(\boldsymbol{q}^e) = \int_0^l (\, \mathcal{T}(\sigma, \boldsymbol{q}^e, \dot{\boldsymbol{q}}^e) - \mathcal{U}(\sigma, \boldsymbol{q}^e)\,)\, L_0\, d\sigma. \tag{66}$$

So far we have not precisely defined the type of loading. Let us assume that a load acting on the element is composed from three additive parts. The first one is the interaction of the neighbored elements. The second one is the external point (concentrated) loadings acting on the nodes. The last one represents a distributed load with fixed direction and prescribed intensity as mentioned in Section 2. In keeping with the load definitions in the principle of virtual work, the total load has to be defined with respect to the inertial basis because the generalized nodal displacements are defined with respect to them. Thus, let us denote

$$\boldsymbol{f}_a^i(\tau) = \begin{bmatrix} f_{xa}^i(\tau) \\ f_{ya}^i(\tau) \\ f_{za}^i(\tau) \end{bmatrix}, \quad \boldsymbol{f}_b^i = \begin{bmatrix} f_{xb}^i(\tau) \\ f_{yb}^i(\tau) \\ f_{zb}^i(\tau) \end{bmatrix}, \qquad \boldsymbol{l}_a^i = \begin{bmatrix} l_{xa}^i(\tau) \\ l_{ya}^i(\tau) \\ l_{za}^i(\tau) \end{bmatrix}, \quad \boldsymbol{l}_b^i = \begin{bmatrix} l_{xb}^i(\tau) \\ l_{yb}^i(\tau) \\ l_{zb}^i(\tau) \end{bmatrix} \tag{67}$$

be the interaction force and torque vector at nodes $\sigma = 0$ and $\sigma = l$ respectively.

Similarly, the external point loadings are expressed as

$$\boldsymbol{f}_a^c(\tau) = \begin{bmatrix} f_{xa}^c(\tau) \\ f_{ya}^c(\tau) \\ f_{za}^c(\tau) \end{bmatrix}, \quad \boldsymbol{f}_b^c(\tau) = \begin{bmatrix} f_{xb}^c(\tau) \\ f_{yb}^c(\tau) \\ f_{zb}^c(\tau) \end{bmatrix}, \qquad \boldsymbol{l}_a^c = \begin{bmatrix} l_{xa}^c(\tau) \\ l_{ya}^c(\tau) \\ l_{za}^c(\tau) \end{bmatrix}, \quad \boldsymbol{l}_b^c = \begin{bmatrix} l_{xb}^c(\tau) \\ l_{yb}^c(\tau) \\ l_{zb}^c(\tau) \end{bmatrix}, \tag{68}$$

while the distributed forces and torques may be expressed as

$$\boldsymbol{\xi}^d = \begin{bmatrix} \xi_x^d(\sigma,\tau) \\ \xi_y^d(\sigma,\tau) \\ \xi_z^d(\sigma,\tau) \end{bmatrix}, \quad \boldsymbol{\eta}^d = \begin{bmatrix} \eta_x^d(\sigma,\tau) \\ \eta_y^d(\sigma,\tau) \\ \eta_z^d(\sigma,\tau) \end{bmatrix}. \tag{69}$$

The virtual work done by the distributed load has the form

$$\begin{aligned} \delta\mathscr{W}^d &= \int_0^l \left(\xi_x^d \delta\bar{x} + \xi_y^d \delta\bar{y} + \xi_z^d \delta\bar{z} + \eta_x^d \delta\phi_x + \eta_y^d \delta\phi_y + \eta_z^d \delta\phi_z \right) L_0 \, d\sigma \\ &= \int_0^l \left(\xi_x^d \frac{\partial \bar{x}(\sigma, \boldsymbol{q}^e)}{\partial \boldsymbol{q}^e} + \xi_y^d \frac{\partial \bar{y}(\sigma, \boldsymbol{q}^e)}{\partial \boldsymbol{q}^e} + \xi_z^d \frac{\partial \bar{z}(\sigma, \boldsymbol{q}^e)}{\partial \boldsymbol{q}^e} + \right. \\ &\quad \left. + \eta_x^d \frac{\partial \phi_x(\sigma, \boldsymbol{q}^e)}{\partial \boldsymbol{q}^e} + \eta_y^d \frac{\partial \phi_y(\sigma, \boldsymbol{q}^e)}{\partial \boldsymbol{q}^e} + \eta_z^d \frac{\partial \phi_z(\sigma, \boldsymbol{q}^e)}{\partial \boldsymbol{q}^e} \right) \delta\boldsymbol{q}^e \, L_0 \, d\sigma \end{aligned} \tag{70}$$

For the sake of convenience, let

$$\boldsymbol{f}^{ie}(\tau) = \begin{bmatrix} \boldsymbol{f}_a^i(\tau) \\ \boldsymbol{l}_a^i(\tau) \\ \boldsymbol{f}_b^i(\tau) \\ \boldsymbol{l}_b^i(\tau) \end{bmatrix}, \quad \boldsymbol{f}^{ce}(\tau) = \begin{bmatrix} \boldsymbol{f}_a^c(\tau) \\ \boldsymbol{l}_a^c(\tau) \\ \boldsymbol{f}_b^c(\tau) \\ \boldsymbol{l}_b^c(\tau) \end{bmatrix}, \tag{71}$$

$$\boldsymbol{f}^{de}(\tau, \boldsymbol{q}^e) = \int_0^l \left(\xi_x^d(\tau) \frac{\partial \bar{x}(\sigma, \boldsymbol{q}^e)}{\partial \boldsymbol{q}^e} + \cdots + \eta_z^d(\tau) \frac{\partial \phi_z(\sigma, \boldsymbol{q}^e)}{\partial \boldsymbol{q}^e} \right)^T L_0 \, d\sigma. \tag{72}$$

Then, the total virtual work done by the three additive parts are

$$\delta\mathscr{W} = (\boldsymbol{f}^{ie} + \boldsymbol{f}^{ce} + \boldsymbol{f}^{de})^T \cdot \delta\boldsymbol{q}^e. \tag{73}$$

Substituting (66) and (73) into (49), taking variations using the chain rule, and integrating by parts, yield the generalized Lagrange equations of motion for the Cosserat rod element:

$$\frac{d}{d\tau}\left(\frac{\partial L}{\partial \dot{q}_j}\right) - \frac{\partial L}{\partial q_j} = f_j^{ie}(\tau) + f_j^{ce}(\tau) + f_j^{de}(\tau, \boldsymbol{q}^e) \tag{74}$$

For a general configuration with nonzero generic nodal displacements $\boldsymbol{q}^e$, the ordinary differential equations of motion with up to third order nonlinearities of displacements and first order kinetic terms can be obtained as

$$\boldsymbol{M}^e\ddot{\boldsymbol{q}}^e + \boldsymbol{K}^e\boldsymbol{q}^e + \boldsymbol{g}^e(\boldsymbol{q}^e) = \boldsymbol{f}^{ie}(\tau) + \boldsymbol{f}^{ce}(\tau) + \boldsymbol{f}^{de}(\tau, \boldsymbol{q}^e), \tag{75}$$

where $\boldsymbol{M}^e$ and $\boldsymbol{K}^e$ are mass and (linear) stiffness matrices of the element model, $\boldsymbol{g}^e(\boldsymbol{q}^e)$ is a nonlinear vector with quadratic and cubic terms of $\boldsymbol{q}^e$. Since the mass of a typical rod, such as the springlike support component of MEMS, is very small comparing with the mass of the main device in practice only the first order kinetic terms are reserved in Equation (75).

The detailed expressions of $\boldsymbol{M}^e$, $\boldsymbol{K}^e$ and $\boldsymbol{g}^e(\boldsymbol{q}^e)$ have been implemented in a MAPLE program [30]. For the sake of illustration, the explicit expressions of $\boldsymbol{M}^e$, $\boldsymbol{K}^e$ and $\boldsymbol{g}^e(\boldsymbol{q}^e)$ for a cantilever beam as a special Cosserat rod element are listed in Appendix.

6 Dynamical Responses of rods by Cosserat Rod Elements

6.1 Assembly of equations of motion for whole system

We could analyze all of the types of systems consist of a set of interconnected components described in the introduction by using Cosserat rod elements for the deformable parts or subdivided members. Two- and three-dimensional frame structures require rotation-of-axes transformation for actions and displacements. For the sake of convenience, in this section we shall examine only the type of structure which is aligned with reference axes, using properties of the Cosserat rod element developed in the preceding sections. The analysis of the response of a number of complex structures is beyond the scope of this paper and will be presented in future publications.

After stiffness, mass, and actual or equivalent nodal loads for individual Cosserat rod element are generated, we can assembly them to form the equations of motion for a whole system. We define global displacement vector $\boldsymbol{q}$ holding the displacement variables for all mesh nodes, such that

$$\boldsymbol{q} = [X_1\ Y_1\ Z_1\ \Phi_{x1}\ \Phi_{y1}\ \Phi_{z1}\ X_2\ Y_2\ Z_2\ \Phi_{x2}\ \Phi_{y2}\ \Phi_{z2}\ \cdots]^T. \tag{76}$$

The equations of motion for the whole system can be constructed by simply adding the contributions from all the elements. In this way, expanding the matrix or operator for each individual element to make

them the same size as the system matrices or operators, we have

$$\boldsymbol{M} = \sum_{i=1}^{n_e} \boldsymbol{M}_i^e, \qquad \boldsymbol{K} = \sum_{i=1}^{n_e} \boldsymbol{K}_i^e, \tag{77}$$

and

$$\boldsymbol{g}(\boldsymbol{q}) = \sum_{i=1}^{n_e} \boldsymbol{g}_i^e(\boldsymbol{q}), \qquad \boldsymbol{f}^c(\tau) = \sum_{i=1}^{n_e} \boldsymbol{f}_i^{ce}(\tau), \qquad \boldsymbol{f}^d(\tau, \boldsymbol{q}) = \sum_{i=1}^{n_e} \boldsymbol{f}_i^{de}(\tau, \boldsymbol{q}). \tag{78}$$

where n_e is the number of elements. In Equation (77) $\boldsymbol{M}$ and $\boldsymbol{K}$ represent the system mass matrix and the system (linear) stiffness matrix. Similarly, the action vectors $\boldsymbol{f}^c(\tau)$ and $\boldsymbol{f}^d(\tau, \boldsymbol{q})$ are actual and equivalent nodal loads for the whole system. The contributions from the interaction forces and torques from all the elements must be of balance and the total action must be vanished. Then the undamped equations of motion for the assembled system become

$$\boldsymbol{M}\ddot{\boldsymbol{q}} + \boldsymbol{K}\boldsymbol{q} + \boldsymbol{g}(\boldsymbol{q}) = \boldsymbol{f}^c(\tau) + \boldsymbol{f}^d(\tau, \boldsymbol{q}). \tag{79}$$

This equation gives the system equations of motion all nodal displacements, regardless of whether they are free or restricted.

In preparation for solving the nonlinear dynamic equations (79), as in the standard finite element procedure, we rearrange and partition it as follows

$$\begin{bmatrix} \boldsymbol{M}_{ff} & \boldsymbol{M}_{fr} \\ \boldsymbol{M}_{rf} & \boldsymbol{M}_{rr} \end{bmatrix} \begin{bmatrix} \ddot{\boldsymbol{q}}_f \\ \ddot{\boldsymbol{q}}_r \end{bmatrix} + \begin{bmatrix} \boldsymbol{K}_{ff} & \boldsymbol{K}_{fr} \\ \boldsymbol{K}_{rf} & \boldsymbol{K}_{rr} \end{bmatrix} \begin{bmatrix} \boldsymbol{q}_f \\ \boldsymbol{q}_r \end{bmatrix} + \begin{bmatrix} \boldsymbol{g}_f(\boldsymbol{q}_f, \boldsymbol{q}_r) \\ \boldsymbol{g}_r(\boldsymbol{q}_f, \boldsymbol{q}_r) \end{bmatrix}$$

$$= \begin{bmatrix} \boldsymbol{f}_f^c(\tau) + \boldsymbol{f}_f^d(\tau, \boldsymbol{q}_f, \boldsymbol{q}_r) \\ \boldsymbol{f}_r^c(\tau) + \boldsymbol{f}_r^d(\tau, \boldsymbol{q}_f, \boldsymbol{q}_r) \end{bmatrix}, \tag{80}$$

in which the subscript f refers to free nodal displacements while the subscript r denotes restrained nodal displacements. If the support motions (at constraints) are zero, the equation (80) can be simplified to

$$\boldsymbol{M}_{ff}\ddot{\boldsymbol{q}}_f + \boldsymbol{K}_{ff}\boldsymbol{q}_f + \boldsymbol{g}_f(\boldsymbol{q}_f) = \boldsymbol{f}_f^c(\tau) + \boldsymbol{f}_f^d(\tau, \boldsymbol{q}_f), \tag{81}$$

and

$$\boldsymbol{M}_{rf}\ddot{\boldsymbol{q}}_f + \boldsymbol{K}_{rf}\boldsymbol{q}_f + \boldsymbol{g}_r(\boldsymbol{q}_f) = \boldsymbol{f}_r^c(\tau) + \boldsymbol{f}_r^d(\tau, \boldsymbol{q}_f), \tag{82}$$

which can be used for solving the free displacements $\boldsymbol{q}_f(\tau)$ and support actions $\boldsymbol{f}_r^c(\tau)$, respectively.

6.2 Simulation results and discussion for a simple cantilever

A cantilever, as shown in Figure 2, is now presented as a simple example to demonstrate high accuracy and excellent performance of the proposed Cosserat rod elements. Numerical calculations based on (81) are carried out for a uniform horizontal cantilever of length $L = 0.3$m, of constant cross section with width $B = 0.01$m and thickness $D = 0.005$m. The mass density and the Young's modulus are assumed to be $\rho = 3.0 \times 10^3$kg/m^3 and $E = 2.08 \times 10^8$Pa.

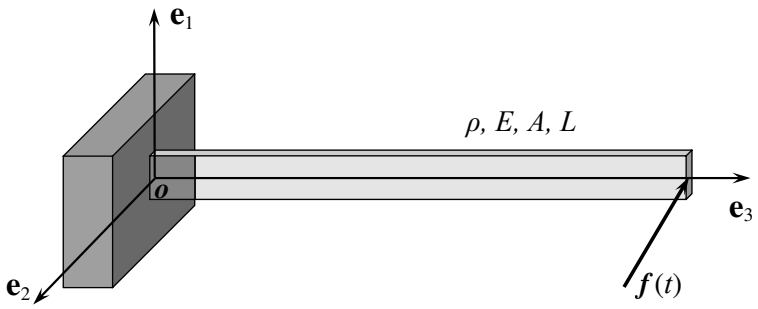

Figure 2: Schematic of a simple Cantilever

Dividing the cantilever into n_e elements of equal length, we can establish the nonlinear differential equations of motion (81) for solving the free displacements. In what follows, the natural frequencies of the linearized system are studied and used to compare with those derived from the classical beam theory presented in textbooks (see, for example [31]), and numerical simulations for the responses of the nonlinear dynamical system (81) under external harmonic excitations are performed with Matlab.

Table 1 Flexural natural frequencies based on CRE approach and exact Continua method

ω_i	Flexural frequencies in $\mathbf{e}_1$-$\mathbf{e}_3$ plane			Flexural frequencies in $\mathbf{e}_2$-$\mathbf{e}_3$ plane		
(rad/sec)	CRE	CBT	|Error| (%)	CRE	CBT	|Error| (%)
1	29.7607	29.7665	0.0197	14.8827	14.8833	0.0036
2	186.358	186.544	0.0995	93.2838	93.2718	0.0129
3	522.329	522.329	0.0000	261.868	261.164	0.2692
4	1028.68	1023.56	0.5005	516.914	511.778	1.0035
5	1707.74	1692.01	0.5155	857.104	846.007	1.3118

First, the flexural natural frequencies calculated in terms of the linearized equations of the nonlinear system (81) obtained by Cosserat element approach, together with the theoretical results obtained by

employing the classical beam theory (CBT) are given in Table 1. The flexural natural frequencies in both $\mathbf{e}_1$-$\mathbf{e}_3$ plane and $\mathbf{e}_2$-$\mathbf{e}_3$ plane, based on the CRE approach, showed their excellent convergency (the corresponding results listed in Table 1 are found, when only five Cosserat rod elements are used).

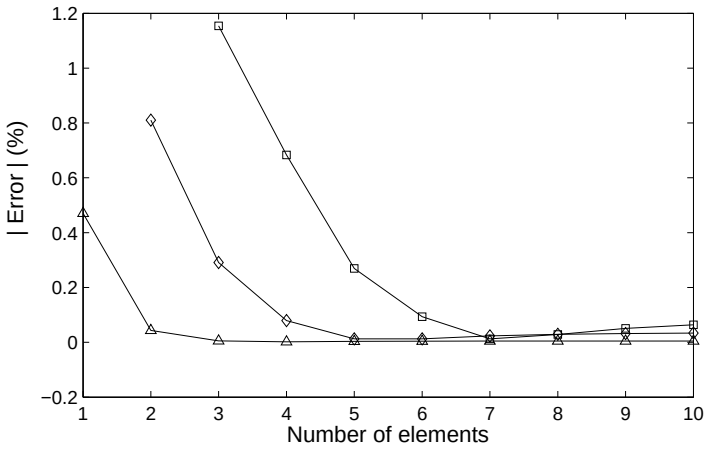

Figure 3: Convergency test for the first flexural frequencies in $\mathbf{e}_2$-$\mathbf{e}_3$ plane. $-\triangle-$, ω_1; $-\Diamond-$, ω_2; $-\square-$, ω_3.

Figure 3 represents the CRE convergency tests corresponding to the first three flexural natural frequencies in $\mathbf{e}_2$-$\mathbf{e}_3$ plane of the rod. As can be seen for the first frequency, the |error| is found to be very small ($\leq 0.1\%$) even when only two elements are used. In fact the |error| for the first frequency is only 0.4535% when just one element is used. For the second and third natural frequencies, the results are converging with approximately 0.1% error, when six elements are used.

In the second part of this example, based on the derived nonlinear system (81), numerical simulations are performed to investigate the dynamic responses of the cantilever under harmonic excitations. The differential equations of motion are full coupled by the nonlinear terms and could exhibit internal resonance introduced by the nonlinearities. They also exhibit external resonances when the external excitation is periodic and the frequency of a component of its Fourier series is near one of the natural frequencies of the system, or near a multiple of a natural frequencies. The detailed analysis of complex dynamic behavior, such as bifurcation and chaos, of the system is not the main focus of this paper. We only compare here the responses of the system, when different number of elements are used.

The displacement and angular time histories of the free end of the cantilever under external loads $f_x^c(t) = 0.01\cos(8t)$, $f_y^c(t) = 0.005\sin(8t)$ and at zero initial conditions are shown in Figure 4 when two elements are used and in Figure 5 when ten elements are used, respectively. It is interesting to note that amplitudes and periods of the responses are very closed in this two situations. To enhance

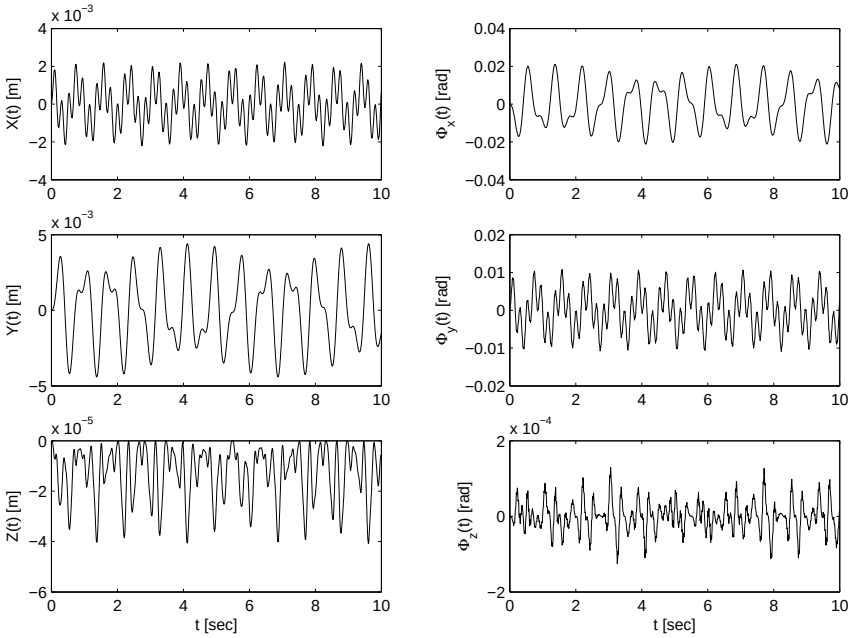

Figure 4: Displacement time histories of the rod with external loads $f_x(t) = 0.01\cos(8 * t)$, $f_y(t) = 0.005\sin(8 * t)$ and zero initial conditions: two elements case.

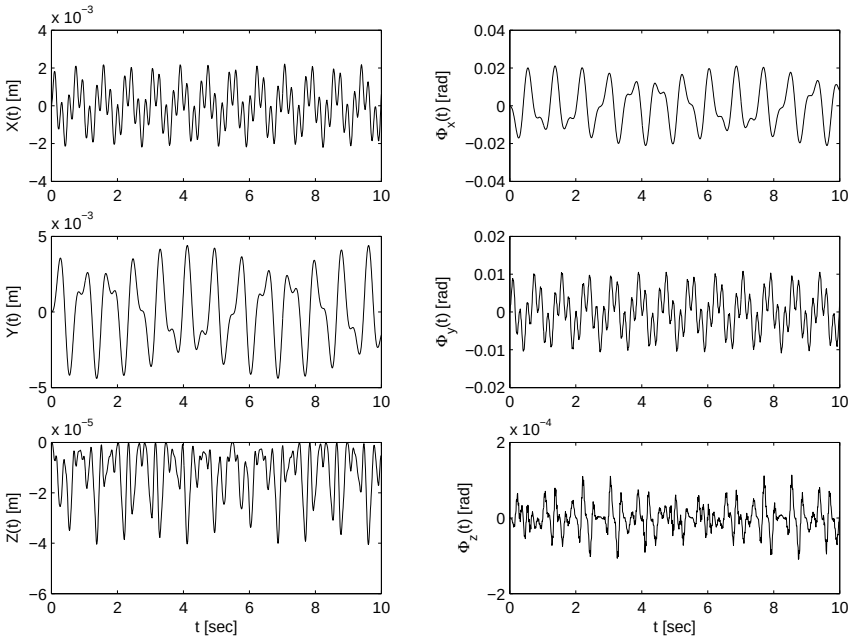

Figure 5: Displacement time histories of the rod with external loads $f_x(t) = 0.01\cos(8 * t)$, $f_y(t) = 0.005\sin(8 * t)$ and zero initial conditions: ten elements case.

this observation, the phase plane diagrams for $Y(t)$–$\dot{Y}(t)$ in four different cases, namely one element, two elements, three elements and ten elements, are plotted in Figure 6 (a), (b), (c) and (d), respectively.

Comparing the four diagrams in Figure 6 shows that the modal when two or three elements are used can exhibit almost the same behavior of the model when ten elements are used.

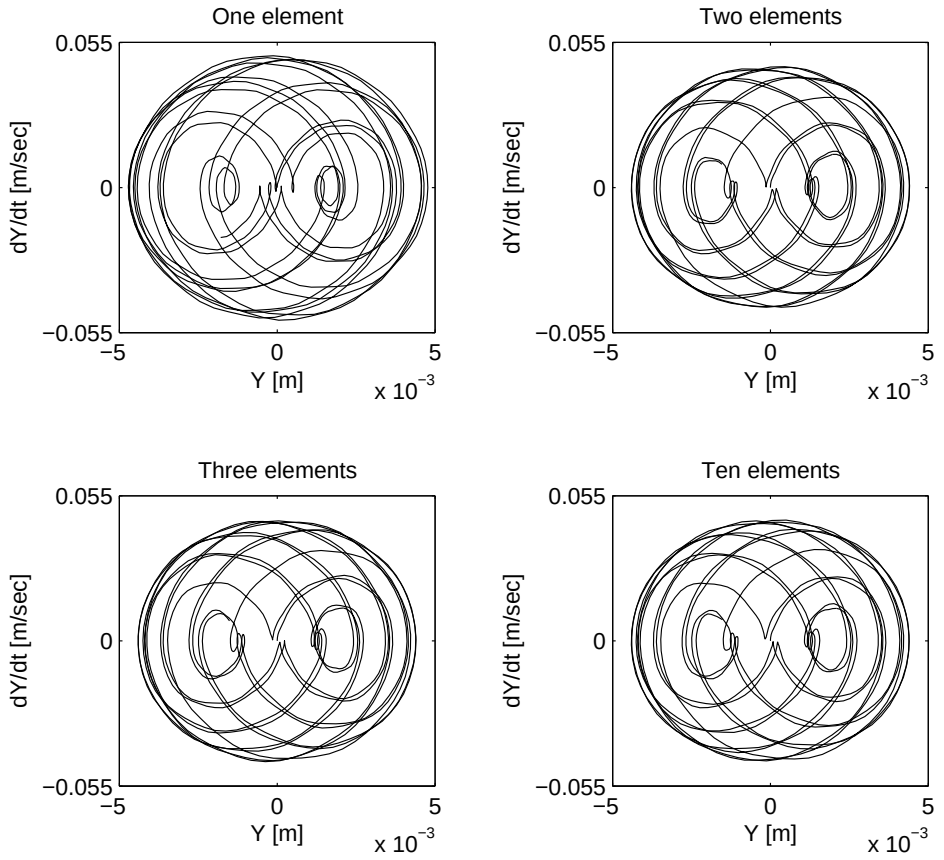

Figure 6: Phase plane diagram of Y–$\dot{Y}$ with external loads $f_x(t) = 0.01\cos(8*t)$, $f_y(t) = 0.005\sin(8*t)$ and zero initial conditions.

According to the analysis of natural frequencies and the analysis of harmonic responses of the established nonlinear dynamic systems, we believe, in practical engineering problem, especial for the structure composed of springlike flexural components such as the device in MEMS, only a few Cosserat rod elements are needed to model a flexural component. For the very slender flexural components, we can even use only one element to model such a component.

7 Conclusion

A Cosserat rod element formulation for the modelling of 3-dimensional dynamics of slender structures has been proposed in this paper. The modelling strategy of this new approach employed the exact nonlin-

ear kinematic relationships in the sense of Cosserat theory, and adopted the Bernoulli hypothesis. Finite displacements and rotations as well as finite extensional, torsional, and bending strains are accounted for. The Kirchoff constitutive relations, which provide an adequate description of elastic properties in terms of a few elastic moduli, are adopted. A deformed configuration of the rod is described by the displacement vector of the deformed centroid curves and an orthonormal moving frame, rigidly attached to the cross-section of the rod. The position of the moving frame relative to the inertial frame is specified by the rotation matrix, parametrized by a rotational vector. The approximation solutions of the nonlinear partial differential equations of motion in quasi-static sense are chosen as the shape functions with up to third order nonlinear terms of generic nodal displacements. This lends the approach very well to achieve higher accuracy of the dynamic responses of the model by dividing the slender rod into a few elements. Based on the Lagrangian constructed by the Cosserat kinetic energy and strain energy expressions, the principle of virtual work is employed to derive the ordinary differential equations of motion with third order nonlinear generic nodal displacements.

A cantilever as a simple example has been presented to illustrate the use of the formulation developed here to obtain the lower order nonlinear ordinary differential equations of motion of a given structure. The natural frequency analysis for the linearized equations and the numerical simulation analysis for the nonlinear model show that in practical engineering problem, especial for the structure composed of springlike flexural components such as the device in MEMS, only a few Cosserat rod elements are needed to model a flexural component.

The mathematical simplicity when formulating deformable components enables more convenient for modelling the multibody systems that consist of interconnected rigid and deformable components. The Cosserat rod element approach therefore is feasible to be used to capture the most significant characteristics of a multi- rigid and deformable body system in a few variables governed by nonlinear ordinary differential equations of motion.

As the first step to present the Cosserat rod element approach, we have limited our attention to the modelling of Cosserat rod elements in which the effect of shear has been neglected. The extension of the present formulation to the modelling of more general Cosserat rod elements in which the finite extensional, torsional, bending strains as well as shear are accounted for is highly desirable.

Acknowledgements The authors are grateful to the EPSRC (Computational Engineering Mathematics Programme) and the EC(Framework Programme) for financial support in this study.

Appendix

Let us assume that a uniform cantilever beam of length L, of constant cross section with area A and density ρ, is fixed at $s = 0$ and free at $s = L$. In this case, we have $\boldsymbol{q}_a = 0$, thus $\boldsymbol{q}^e = \boldsymbol{q}_b$. Consequently, $\boldsymbol{M}^e$, $\boldsymbol{K}^e$ become 6×6 matrices, and $\boldsymbol{g}^e(\boldsymbol{q}^e)$ is a six dimensional nonlinear vectorial functions of $\boldsymbol{q}^e = \boldsymbol{q}_b$. They are

$$\boldsymbol{M}^e = \begin{bmatrix} \frac{13\mu l^2 + 42I_{22}}{35l} & 0 & 0 & 0 & -\frac{I_{22}}{10} - \frac{11\mu l^2}{210} & 0 \\ 0 & \frac{13\mu l^2 + 42I_{11}}{35l} & 0 & \frac{I_{11}}{10} + \frac{11\mu l^2}{210} & 0 & 0 \\ 0 & 0 & \frac{\mu l}{3} & 0 & 0 & 0 \\ 0 & \frac{I_{11}}{10} + \frac{11\mu l^2}{210} & 0 & \frac{2I_{11}l}{15} + \frac{\mu l^3}{105} & 0 & 0 \\ -\frac{I_{22}}{10} - \frac{11\mu l^2}{210} & 0 & 0 & 0 & \frac{2I_{22}l}{15} + \frac{\mu l^3}{105} & 0 \\ 0 & 0 & 0 & 0 & 0 & \frac{I_{33}l}{3} \end{bmatrix}, \tag{83}$$

$$\boldsymbol{K}_c^e = \begin{bmatrix} \frac{12J_{22}}{l^3} & 0 & 0 & 0 & -\frac{6J_{22}}{l^2} & 0 \\ 0 & \frac{12J_{11}}{l^3} & 0 & \frac{6J_{11}}{l^2} & 0 & 0 \\ 0 & 0 & \frac{K_{33}}{l} & 0 & 0 & 0 \\ 0 & \frac{6J_{11}}{l^2} & 0 & \frac{4J_{11}}{l} & 0 & 0 \\ -\frac{6J_{22}}{l^2} & 0 & 0 & 0 & \frac{4J_{22}}{l} & 0 \\ 0 & 0 & 0 & 0 & 0 & \frac{J_{33}}{l} \end{bmatrix}, \tag{84}$$

and

$$\begin{aligned} g_1(\boldsymbol{q}^e) &= g_{1,1}X_bZ_b + g_{1,2}Y_b\Phi_{zb} + g_{1,3}Z_b\Phi_{yb} + g_{1,4}\Phi_{xb}\Phi_{zb} + g_{1,5}X_b^3 + g_{1,6}X_b^2\Phi_{yb} \\ &\quad + g_{1,7}X_bY_b^2 + g_{1,8}X_bY_b\Phi_{xb} + g_{1,9}X_bZ_b^2 + g_{1,10}X_b\Phi_{xb}^2 + g_{1,11}X_b\Phi_{yb}^2 \\ &\quad + g_{1,12}X_b\Phi_{zb}^2 + g_{1,13}Y_b^2\Phi_{yb} + g_{1,14}Y_bZ_b\Phi_{zb} + g_{1,15}Y_b\Phi_{xb}\Phi_{yb} + g_{1,16}Z_b^2\Phi_{yb} \\ &\quad + g_{1,17}Z_b\Phi_{xb}\Phi_{zb} + g_{1,18}\Phi_{xb}^2\Phi_{zb} + g_{1,19}\Phi_{yb}^3 + g_{1,20}\Phi_{yb}\Phi_{zb}^2\,, \end{aligned} \tag{85}$$

$$\begin{aligned} g_2(\boldsymbol{q}^e) &= g_{2,1}X_b\Phi_{zb} + g_{2,2}Y_bZ_b + g_{2,3}Z_b\Phi_{xb} + g_{2,4}\Phi_{yb}\Phi_{zb} + g_{2,5}X_b^2Y_b + g_{2,6}X_b^2\Phi_{xb}, \\ &\quad + g_{2,7}X_bY_b\Phi_{yb} + g_{2,8}X_bZ_b\Phi_{zb} + g_{2,9}X_b\Phi_{xb}\Phi_{yb} + g_{2,10}Y_b^3 + g_{2,11}Y_b^2\Phi_{xb} \\ &\quad + g_{2,12}Y_bZ_b^2 + g_{2,13}Y_b\Phi_{xb}^2 + g_{2,14}Y_b\Phi_{yb}^2 + g_{2,15}Y_b\Phi_{zb}^2 + g_{2,16}Z_b^2\Phi_{xb} \\ &\quad + g_{2,17}Z_b\Phi_{yb}\Phi_{zb} + g_{2,18}\Phi_{xb}^3 + g_{2,19}\Phi_{xb}\Phi_{yb}^2 + g_{2,20}\Phi_{xb}\Phi_{zb}^2\,, \end{aligned} \tag{86}$$

$$
\begin{aligned}
g_3(\boldsymbol{q}^e) &= g_{3,1}X_b^2 + g_{3,2}X_b\Phi_{yb} + g_{3,3}Y_b^2 + g_{3,4}Y_b\Phi_{xb} + g_{3,5}\Phi_{xb}^2 + g_{3,6}\Phi_{yb}^2 + g_{3,7}X_b^2Z_b \\
&\quad + g_{3,8}X_bY_b\Phi_{zb} + g_{3,9}X_bZ_b\Phi_{yb} + g_{3,10}X_b\Phi_{xb}\Phi_{zb} + g_{3,11}Y_b^2Z_b + g_{3,12}Y_bZ_b\Phi_{xb} \\
&\quad + g_{3,13}Y_b\Phi_{yb}\Phi_{zb} + g_{3,14}Z_b\Phi_{xb}^2 + g_{3,15}Z_b\Phi_{yb}^2 + g_{3,16}\Phi_{xb}\Phi_{yb}\Phi_{zb}\,, \qquad (87)
\end{aligned}
$$

$$
\begin{aligned}
g_4(\boldsymbol{q}^e) &= g_{4,1}X_b\Phi_{zb} + g_{4,2}Y_bZ_b + g_{4,3}Z_b\Phi_{xb} + g_{4,4}\Phi_{yb}\Phi_{zb} + g_{4,5}X_b^2Y_b + g_{4,6}X_b^2\Phi_{xb} \\
&\quad + g_{4,7}X_bY_b\Phi_{yb} + g_{4,8}X_bZ_b\Phi_{zb} + g_{4,9}X_b\Phi_{xb}\Phi_{yb} + g_{4,10}Y_b^3 + g_{4,11}Y_b^2\Phi_{xb} \\
&\quad + g_{4,12}Y_bZ_b^2 + g_{4,13}Y_b\Phi_{xb}^2 + g_{4,14}Y_b\Phi_{yb}^2 + g_{4,15}Y_b\Phi_{zb}^2 + g_{4,16}Z_b^2\Phi_{xb} \\
&\quad + g_{4,17}Z_b\Phi_{yb}\Phi_{zb} + g_{4,18}\Phi_{xb}^3 + g_{4,19}\Phi_{xb}\Phi_{yb}^2 + g_{4,20}\Phi_{xb}\Phi_{zb}^2\,, \qquad (88)
\end{aligned}
$$

$$
\begin{aligned}
g_5(\boldsymbol{q}^e) &= g_{1,1}X_bZ_b + g_{5,2}Y_b\Phi_{zb} + g_{5,3}Z_b\Phi_{yb} + g_{5,4}\Phi_{xb}\Phi_{zb} + g_{5,5}X_b^3 + g_{5,6}X_b^2\Phi_{yb} \\
&\quad + g_{5,7}X_bY_b^2 + g_{5,8}X_bY_b\Phi_{xb} + g_{5,9}X_bZ_b^2 + g_{1,10}X_b\Phi_{xb}^2 + g_{1,11}X_b\Phi_{yb}^2 \\
&\quad + g_{5,12}X_b\Phi_{zb}^2 + g5,13Y_b^2\Phi_{yb} + g_{5,14}Y_bZ_b\Phi_{zb} + g_{5,15}Y_b\Phi_{xb}\Phi_{yb} + g_{5,16}Z_b^2\Phi_{yb} \\
&\quad + g_{5,17}Z_b\Phi_{xb}\Phi_{zb} + g_{5,18}\Phi_{xb}^2\Phi_{zb} + g_{5,19}\Phi_{yb}^3 + g_{5,20}\Phi_{yb}\Phi_{zb}^2\,, \qquad (89)
\end{aligned}
$$

$$
\begin{aligned}
g_6(\boldsymbol{q}^e) &= g_{6,1}X_bY_b + g_{6,2}X_b\Phi_{xb} + g_{6,3}Y_b\Phi_{yb} + g_{6,4}\Phi_{xb}\Phi_{yb} + g_{6,5}x_2^2\Phi_{zb} + g_{6,6}X_bY_bZ_b \\
&\quad + g_{6,7}X_bZ_b\Phi_{xb} + g_{6,8}X_b\Phi_{yb}\Phi_{zb} + g_{6,9}Y_b^2\Phi_{zb} + g_{6,10}Y_bZ_b\Phi_{yb} + g_{6,11}Y_b\Phi xb\Phi zb \\
&\quad + g_{6,12}Z_b\Phi_{xb}\Phi_{yb} + g_{6,13}\Phi_{xb}^2\Phi_{zb} + g_{6,14}\Phi_{yb}^2\Phi_{zb}\,, \qquad (90)
\end{aligned}
$$

where, the coefficients of second order nonlinear terms are specified as:

$$
\begin{aligned}
&g_{1,1} = 2g_{3,1} = \frac{6(K_{33}l^2 - 20J_{22})}{5l^4}, && g_{1,2} = g_{2,1} = g_{6,1} = \frac{6(J_{22} - J_{11})}{l^3}, \\
&g_{1,3} = g_{3,2} = -g_{5,1} = \frac{K_{33}l^2 - 60J_{22}}{10l^3}, && g_{1,4} = g_{4,1} = -g_{6,2} = \frac{4J_{11} - J_{22} - J_{33}}{l^2}, \\
&g_{2,2} = 2g_{3,3} = \frac{6(K_{33}l^2 - 20J_{11})}{5l^4}, && g_{2,3} = g_{3,4} = g_{4,2} = \frac{K_{33}l^2 - 60J_{11}}{10l^3}, \\
&g_{2,4} = -g_{5,2} = g_{6,3} = \frac{J_{11} - 4J_{22} + J_{33}}{l^2}, && g_{3,5} = g_{3,6} = \tfrac{1}{2}g_{4,3} = -\tfrac{1}{2}g_{5,3} = \frac{K_{33}}{15}, \\
&g_{4,4} = -g_{5,4} = g_{6,4} = \frac{J_{11} - J_{22}}{l}.
\end{aligned}
$$

The coefficients of third order nonlinear terms are specified as :

$$
\begin{aligned}
g_{1,5} &= \frac{18(7K_{33}^2l^4 - 160J_{22}K_{33}l^2 - 560J_{22}^2)}{175K_{33}l^7}\,, \\
g_{1,6} &= \frac{9(7K_{33}^2l^4 - 260J_{22}K_{33}l^2 - 3360J_{22}^2)}{350K_{33}l^6}\,, \\
g_{1,7} &= \frac{18(7K_{33}l^2 - 80(J_{11} + J_{22}))}{175l^5} - \frac{18(10K_{33}l^2(J_{11} - J_{22})^2 + 112J_{11}J_{22}J_{33})}{35J_{33}K_{33}l^7}\,, \\
g_{1,8} &= \frac{3(7K_{33}l^2 - 480J_{11} + 220J_{22})}{175l^4} - \frac{18(10K_{33}l^2(J_{11} - J_{22})^2 + 112J_{11}J_{22}J_{33})}{35J_{33}K_{33}l^6}\,,
\end{aligned}
$$

$$g_{1,9} = -\frac{K_{33}^2 l^4 + 840 J_{22} K_{33} - 25200 J_{22}^2}{700 J_{22} l^5} \,,$$

$$g_{1,10} = \frac{14 K_{33} l^2 - 500 J_{11} - 80 J_{22} + 175 J_{33}}{175 l^3} - \frac{52 K_{33} l^2 (J_{11} - J_{22})^2 + 504 J_{11} J_{22} J_{33}}{35 J_{33} K_{33} l^5} \,,$$

$$g_{1,11} = \frac{63 K_{33}^2 l^4 - 520 J_{22} K_{33} l^2 - 38640 J_{22}^2}{700 K_{33} l^5} \,,$$

$$g_{1,12} = \frac{20 J_{11}^2 - 16 J_{11} J_{22} - 4 J_{11} J_{33} - 4 J_{22}^2 + 4 J_{22} J_{33} - J_{33}^2}{5 J_{11} l^3} \,,$$

$$g_{1,13} = -\frac{3(7 K_{33} l^2 - 480 J_{22} + 220 J_{11})}{350 l^4} + \frac{9(10 K_{33} l^2 (J_{11} - J_{22})^2 + 112 J_{11} J_{22} J_{33})}{35 J_{33} K_{33} l^6} \,,$$

$$g_{1,14} = \frac{12(J_{11} - J_{22})}{l^4} \,,$$

$$g_{1,15} = -\frac{7 K_{33} l^2 + 900(J_{11} + J_{22}) - 700 J_{33}}{700 l^3} + \frac{118 K_{33} l^2 (J_{11} - J_{22})^2 + 1428 J_{11} J_{22} J_{33}}{35 J_{33} K_{33} l^5} \,,$$

$$g_{1,16} = \frac{K_{33}^2 l^4 - 8400 J_{22}^2}{1400 J_{22} l^4} \,,$$

$$g_{1,17} = -\frac{5 J_{11} K_{33} l^2 - 2 J_{22} K_{33} l^2 + J_{33} K_{33} l^2 - 240 J_{11}^2 + 60 J_{11} J_{22} + 60 J_{11} J_{33}}{60 J_{11} l^3} \,,$$

$$g_{1,18} = -\frac{7 K_{33} l^2 - 240 J_{11} - 30 J_{22}}{1050 l^2} + \frac{40 K_{33} l^2 (J_{11} - J_{22})^2 + 462 J_{11} J_{22} J_{33}}{35 J_{33} K_{33} l^4} \,,$$

$$g_{1,19} = -\frac{7 K_{33} l^4 - 270 J_{22} K_{33} l^2 - 13860 J_{22}^2}{1050 K_{33} l^4} \,,$$

$$g_{1,20} = -\frac{10 J_{11}^2 - 16 J_{11} J_{22} + J_{11} J_{33} - 4 J_{22}^2 + 4 J_{22} J_{33} - J_{33}^2}{10 J_{11} l^2};$$

$$g_{2,7} = -\frac{6(7 K_{33} l^2 - 480 J_{22} + 220 J_{11})}{350 l^4} + \frac{18(10 K_{33} l^2 (J_{11} - J_{22})^2 + 112 J_{11} J_{22} J_{33})}{35 J_{33} K_{33} l^6} \,,$$

$$g_{2,10} = \frac{18(7 K_{33}^2 l^4 - 160 J_{11} K_{33} l^2 - 560 J_{11}^2)}{175 K_{33} l^7} \,,$$

$$g_{2,11} = \frac{9(7 K_{33}^2 l^4 - 260 J_{11} K_{33} l^2 - 3360 J_{11}^2)}{350 K_{33} l^6} \,,$$

$$g_{2,12} = -\frac{K_{33}^2 l^4 + 840 J_{11} K_{33} - 25200 J_{11}^2}{700 J_{11} l^5} \,,$$

$$g_{2,13} = \frac{63 K_{33}^2 l^4 - 520 J_{11} K_{33} l^2 - 38640 J_{11}^2}{700 K_{33} l^5} \,,$$

$$g_{2,14} = \frac{14 K_{33} l^2 - 500 J_{22} - 80 J_{11} + 175 J_{33}}{175 J_{33} K_{33} l^5} - \frac{52 K_{33} l^2 (J_{11} - J_{22})^2 + 504 J_{11} J_{22} J_{33}}{35 J_{33} K_{33} l^5} \,,$$

$$g_{2,15} = \frac{20 J_{22}^2 - 16 J_{11} J_{22} - 4 J_{22} J_{33} - 4 J_{11}^2 + 4 J_{11} J_{33} - J_{33}^2}{5 J_{22} l^3} \,,$$

$$g_{2,16} = -\frac{K_{33}^2 l^4 - 8400 J_{11}^2}{1400 J_{11} l^4} \,,$$

$$g_{2,17} = -\frac{5J_{22}K_{33}l^2 - 2J_{11}K_{33}l^2 + J_{33}K_{33}l^2 - 240J_{22}^2 + 60J_{11}J_{22} + 60J_{22}J_{33}}{60J_{22}l^3} ,$$

$$g_{2,18} = \frac{7K_{33}l^4 - 270J_{11}K_{33}l^2 - 13860J_{11}^2}{1050K_{33}l^4} ,$$

$$g_{2,19} = \frac{7K_{33}l^2 - 240J_{22} - 30J_{11}}{1050l^2} - \frac{40K_{33}l^2(J_{11} - J_{22})^2 + 462J_{11}J_{22}J_{33}}{35l^2} ,$$

$$g_{2,20} = \frac{10J_{22}^2 - 16J_{11}J_{22} + J_{22}J_{33} - 4J_{11}^2 + 4J_{11}J_{33} - J_{33}^2}{10J_{22}l^2} ,$$

$$g_{3,14} = -\frac{K_{33}(11K_{33}l^2 - 840J_{11})}{6300J_{11}l} ,$$

$$g_{3,15} = -\frac{K_{33}(11K_{33}l^2 - 840J_{22})}{6300J_{22}l} ,$$

$$g_{3,16} = \frac{K_{33}(2J_{11}^2 - J_{11}J_{33} - 2J_{22}^2 + J_{22}J_{33})}{120J_{11}J_{22}} ,$$

$$g_{4,18} = \frac{7K_{33}l^4 - 180J_{11}K_{33}l^2 - 7560J_{11}^2}{1575K_{33}l^3} ,$$

$$g_{4,19} = \frac{14K_{33}l^2 - 180(J_{11} + J_{22}) + 175J_{33}}{1575l} - \frac{285K_{33}l^2(J_{11} - J_{22})^2 + 3024J_{11}J_{22}J_{33}}{315J_{33}K_{33}l^3} ,$$

$$g_{4,18} = \frac{12J_{11}^2 + 28J_{11}J_{22} - 12J_{11}J_{33} - 20J_{22}^2 + 2J_{22}J_{33} + 3J_{33}^2}{60J_{22}l} ,$$

$$g_{5,19} = -\frac{7K_{33}l^4 - 180J_{22}K_{33}l^2 - 7560J_{22}^2}{1575K_{33}l^3} ,$$

$$g_{5,20} = -\frac{12J_{22}^2 + 28J_{11}J_{22} - 12J_{22}J_{33} - 20J_{11}^2 + 2J_{11}J_{33} + 3J_{33}^2}{60J_{11}l} ,$$

and

$$g_{2,5} = g_{1,7}, \quad g_{2,6} = \tfrac{1}{2}g_{1,8}, \quad g_{2,8} = g_{1,14}, \quad g_{2,9} = g_{1,15}, \quad g_{3,7} = g_{1,9},$$

$$g_{3,8} = g_{1,14}, \quad g_{3,9} = \tfrac{1}{2}g_{1,16}, \quad g_{3,10} = g_{1,17}, \quad g_{3,11} = g_{2,12}, \quad g_{3,12} = 2g_{1,16},$$

$$g_{3,13} = -g_{2,17}, \quad g_{4,5} = \tfrac{1}{2}g_{1,8}, \quad g_{4,6} = g_{1,10}, \quad g_{4,7} = g_{1,15}, \quad g_{4,8} = g_{1,17},$$

$$g_{4,9} = 3g_{1,18}, \quad g_{4,10} = -\tfrac{1}{3}g_{2,11}, \quad g_{4,11} = g_{2,13}, \quad g_{4,12} = g_{2,16}, \quad g_{4,13} = 3g_{2,18},$$

$$g_{4,14} = g_{2,19}, \quad g_{4,15} = g_{2,20}, \quad g_{4,16} = g_{3,14}, \quad g_{4,17} = g_{3,16}, \quad g_{5,5} = \tfrac{1}{3}g_{1,6},$$

$$g_{5,6} = -g_{1,11}, \quad g_{5,7} = -\tfrac{1}{2}g_{2,7}, \quad g_{5,8} = -g_{1,15}, \quad g_{5,9} = -g_{1,16}, \quad g_{5,10} = -g_{1,18},$$

$$g_{5,11} = -3g_{1,19}, \quad g_{5,12} = -g_{1,20}, \quad g_{5,13} = -g_{2,14}, \quad g_{5,14} = -g_{2,17}, \quad g_{5,15} = -g_{2,19},$$

$$g_{5,16} = g_{3,15}, \quad g_{5,17} = -g_{3,16}, \quad g_{5,18} = -g_{4,19}, \quad g_{6,5} = g_{1,12}, \quad g_{6,6} = g_{1,14},$$

$$g_{6,7} = g_{1,17}, \quad g_{6,8} = 2g_{1,20}, \quad g_{6,9} = g_{2,15}, \quad g_{6,10} = -g_{3,13}, \quad g_{6,11} = 2g_{2,20},$$

$$g_{6,12} = g_{3,16}, \quad g_{6,13} = -g_{4,20}, \quad g_{6,14} = g_{5,20}.$$

References

[1] J.H. Argyris, P.C. Dunne, G. Malejannakis and D.W. Scharpf. On large displacements–small strain analysis of structures with rotational degree of freedom. Computer Methods in Applied Mechanics and Engineering 14 (1978) 99-135.

[2] A. Cardona and M. Geradin. A beam finite element non-linear theory with finite rotations. International Journal for Numerical Methods in Engineering 26 (1988) 2403-2438.

[3] A. Dutta and D.W. White. Large displacement formulation of a three-dimensional beam element with cross-sectional warping. Computers and Structures 45 (1992) 9-24.

[4] A.A. Shabana. Dynamics of Multibody Systems. Camberidge, Combridge University Press, Second Edition, 1998.

[5] T. Belytschko, W.K. Liu and B. Moran. Nonlinear Finite Elements for Continua and Structures. Chichester, John Wiley & Sons, Ltd., 2002.

[6] A.E. Green, P.M. Naghdi and M.L. Wenner. On the theory of rods I: derivations from the three-dimensional equations. Proceedings of the Royal Society, London A 337 (1974) 451-483.

[7] S.S. Antman. Nonlinear Problems of Elasticity. Applied Mathematical Sciences 107, New York: Springer-Verlag (1995).

[8] R.W. Tucker and C. Wang. An integrated model for drill-string dynamics. Journal of Sound and Vibration, 224 (1999) 123-165.

[9] S.S. Antman, R.S. Marlow and C.T. Vlahacos. The complicated dynamics of heavy rigid bodies attached to deformable rods. Quarterly of Applied Mathematics 56 (1998) 431-460.

[10] E. Reissner. On finite deformation of space-curved beams. Journal of Applied Mathematics and Physics 32 (1981) 734-744.

[11] J.C. Simo. A finite strain beam formulation – the three-dimensional dynamic problem part I. Computer Methods in Applied Mechanics and Engineering 49 (1985) 55-70.

[12] S.S. Antman. The Theory of Rods. In: Handbuch der Phyik VIa/2, C. Truesdell ed., Berlin: Springer-Verlag (1972) 641-703.

[13] J.C. Simo and L. Vu-Quoc. A three-dimensional finite strain rod model part II: computational aspects. Computer Methods in Applied Mechanics and Engineering 58 (1986) 79-116.

[14] G. Jelenic and M. Saje. A kinematically exact space finite strain beam model – finite element formulation by generalized virtual work principle. Computer Methods in Applied Mechanics and Engineering 120 (1995) 131-161.

[15] W.M. Smolenski. Statically and kinematically exact nonlinear theory of rods and its numerical verification. Computer Methods in Applied Mechanics and Engineering 178 (1999) 89-113.

[16] D. Zupan and M. Saje. Finite-element formulation of geometrically exact three-dimensional beam thoeories based on interpolation of strain measures. Computer Methods in Applied Mechanics and Engineering 192 (2003) 5209-5248.

[17] C.Z. Wozniak. Equations of motion and laws of conservation in the discrete elasticity. Archives of Mechanics 25 (1973) 155-163.

[18] H. Cohen and R.G. Muncaster. The dynamics of pseudo-rigid bodies: general structure and exact solutions. Journal of Elasticity 14 (1984) 127-145.

[19] M.B.Rubin. On the theory of a Cosserat point and its application to the numerical solution of continuum problems. ASME Jornal of Applied Mechanics 52 (1985) 368-372.

[20] M.B.Rubin. On the numerical solusion of one-dimensional continuum problems using the theory of a Cosserat point. ASME Jornal of Applied Mechanics 52 (1985) 373-378.

[21] M.B.Rubin. On the numerical solution of nonlinear string problems using theory of a Cosserat point. International Journal of Solids and Structures 23 (1987) 335-349.

[22] M.B. Rubin. Numerical solution procedures for nonlinear elastic rods using the theory of a Cosserat point. Internatioanl Journal of Solids and Structures 38 (2001) 4395-4437.

[23] G. Lorenz and R. Neual. Network-type modeling of micromachined sensor systems. Proceedings of the International Conference on Modeling and Simulation of Microsystems, Semiconductors, Sensors and Actuators, MSM98, Santa Clara , (1998) 233-238.

[24] T. Mukherjee, G.K. Feder, and R.D. Blanton. Hierarchical design and test of integrated microsystems. IEEE Design and Test of Computers, 16(4) (1999) 18-27.

[25] C. Wang, D. Liu, R. Rosing, A. Richardson and B. De Masi. Construction of nonlinear dynamic MEMS component models using Cosserat theory. Analog Integrated Circuits and Signal Processing, 40 (2004) 117-130.

[26] T. Gould and C.Wang. MEMS beams with defects: a model of non-ideal rods using Cosserat Approach for component level modelling. Journal of Micromechanics and Microengineering 15 (2005) 76-80.

[27] J. Stuelpnagel. On the parametrization of the three-dimensional rotation group. SIAM Review 6 (1964) 422-430.

[28] A. Jones, A. Gray and R. Hutton. Manifolds and Mechanics. Camberidge, Combridge University Press, (1987).

[29] G. Arfken. Mathematical Methods for Physicists. San Fiego, Academic Press, Inc. (1985).

[30] C. Wang, D. Liu and D. Q. Cao. The programm of modelling Cosserat rod elements: I. Shape_Functions.mpl, II. Nonlinear_Stiffness.mpl. Lancaster University, MAPLE code (2004).

[31] J. H. Ginsberg. Mechanical and Structural Vibrations: Theory and Applications. New York: John Wiley and Sons, Inc., 2001.